Analog and digital simulation of line-energizing overvoltages and comparison with measurements in a 400 kV network

tu/e
Research Report
ISSN 0167-9708
Coden: TEUEDE

Eindhoven
University of Technology
Netherlands

Faculty of Electrical Engineering

Analog and Digital Simulation of Line-Energizing Overvoltages and Comparison with Measurements in a 400 kV Network

by
W.F.J. Kersten and G.A.P. Jacobs

EUT Report 88-E-193
ISBN 90-6144-193-5
September 1988

Eindhoven University of Technology Research Reports

EINDHOVEN UNIVERSITY OF TECHNOLOGY

Faculty of Electrical Engineering
Eindhoven The Netherlands

ISSN 0167- 9708 Coden: TEUEDE

ANALOG AND DIGITAL SIMULATION OF LINE-ENERGIZING OVERVOLTAGES AND COMPARISON WITH MEASUREMENTS IN A 400 kV NETWORK

by

W.F.J. Kersten
and
G.A.P. Jacobs

EUT Report 88-E-193
ISBN 90-6144-193-5

Eindhoven
September 1988

CIP-GEGEVENS KONINKLIJKE BIBLIOTHEEK, DEN HAAG

Kersten, W.F.J.

Analog and digital simulation of line-energizing overvoltages
and comparison with measurements in a 400 kV network / by W.F.J.
Kersten and G.A.P. Jacobs. - Eindhoven: University of Technology,
Faculty of Electrical Engineering. - Fig., tab. - (EUT report,
ISSN 0167-9708; 88-E-193)
Met lit. opg., reg.
ISBN 90-6144-193-5
SISO 661.5 UDC 621.311.1.015.3.001.57 NUGI 832
Trefw.: elektriciteitsnetten / elektrische overgangsverschijnselen.

Abstract

Results of line-energization tests in the Dutch 400 kV network have been used as reference for the development of analog and digital simulation techniques to model complex networks for switching transients . In this report transient waveforms and overvoltage peak values obtained through duplication of the line energizations by means of a Transient Network Analyzer and the ElectroMagnetic Transient Program , are presented and compared with field test records . The best resemblance of waveforms has been obtained by EMTP while the cumulative distribution of overvoltage peak values from TNA simulation shows the best match with the field measurements . The statistical overvoltages derived from field tests and simulations are all in the range 1.95 p.u. ± 5 % . The results indicate that both EMTP and TNA are suitable to study switching transients being expected in real networks .

Kersten , W.F.J. and G.A.P. Jacobs
Analog and digital simulation of line-energizing overvoltages and comparison with measurements in a 400 kV network .
Faculty of Electrical Engineering ,
Eindhoven University of Technology , 1988 .
EUT Report 88-E-193

Address of the authors :
ir. W.F.J. Kersten ,
Section Electrical Energy Systems ,
Faculty of Electrical Engineering ,
Eindhoven University of Technology ,
P.O. Box 513 ,
5600 MB Eindhoven ,
the Netherlands

Acknowledgement

The authors wish to thank the N.V. KEMA , Arnhem , Netherlands ,for providing the results of the field tests . Thanks are due also to ir. M.H.J. Bollen and C.M. van der Wouw of the Eindhoven University of Technology for their assistance during the simulations and during the realization of this report .

Contents

1 Introduction

The insulation of components of a power transmission system is stressed not only by the normal operating voltage but in a higher extent by over -voltages originating from lightning discharges , switching operations and faults . The internationally accepted procedures to select the insulation level for systems operating at voltages above 300 kV are mainly based on the magnitude of the switching overvoltages . They presuppose knowledge of the magnitude and frequency of occurance of the switching overvoltages to be expected as those caused by the energization of unloaded overhead lines . This applies especially to systems with overhead lines well-shielded against dangerous lightning strokes to phase conductors , as in the Netherlands .

In the last twenty years much research has been directed to the prediction of switching overvoltages by both transient network analyzers (TNA) and digital computer programs like EMTP . The methods of computation and the simulation of network components have been extensively studied , particularly by Cigré Working Groups [1,2,3,4]. A guide for representation of network elements when calculating transients will soon be presented by WG 33.02 [5] .

Despite the worldwide experience with the application of TNA 's and digital computer programs , there still exists the need of carrying out field tests in real systems [6] . Duplication of these tests offers the possibility to access the validity and limitations of the simulation techniques applied . Just recently EPRI has started a project to gather available comparisons between field tests and EMTP calculations . They will be classified and published as a users reference manual . In this manual also results of the study presented in this report will be summarized .

1.1 Scope of the work

In 1979 N.V. KEMA (Arnhem) has performed field tests in the interconnected Dutch 400 kV network . A number of these tests concerned the energization of one circuit of the double-circuit line Diemen-Krimpen in substation Diemen . Useful data and plots of the open-end voltages in Krimpen during 13 energizing operations has been obtained [7,8] . These have been used as reference material in a research project on switching transients .

The main objective of the project was the development of analog- and digital simulation techniques to model complex networks for switching transients . A number of students participated in this project in fulfilment of their M.Sc. degree . For the TNA new line models were constructed and network reduction techniques were tested [9,10,11] . Also a computer program was developed as , at that time , no facilities to run EMTP were available . In this program , limited to switching- and fault transients , recursive convolution techniques have been applied in simulating the network outside the switched or faulted line by means of Foster equivalent circuits [12,13] . Later on hardware to run EMTP version M39 has been installed . This offered the possibility to duplicate the field tests by EMTP calculations and to compare the various simulation results .

In this report results of KEMA 's field tests and the results of accurate duplication of these tests by EMTP calculations and former TNA simulations are presented .

2 Results of KEMA field tests [7,8]

The network configuration during the field tests is shown in Figure 1 . One circuit of the double-circuit line Diemen-Krimpen , length 57.7 km, was energized 13 times in substation Diemen through circuit-breakers without pre-insertion resistors . The switching operations were executed at random moments of the power frequency cycle. The open end phase-to-ground voltages in Krimpen were registered by means of an analog-digital measuring system (6 channels , 10 bit , 4 k) . The tests have been numbered K1 , K3 - K14 . A typical record of receiving-end overvoltages in Krimpen is shown in Figure 2 . In this test K6 , a maximum overvoltage of 612 kV corresponding to 1.75 p.u. was measured in the first energized phase R . In Table 1 the overvoltage peak-values of all tests have been listed . The mean value is 1.46 p.u. whereas the standard deviation is 0.197 p.u. (Gaussian distribution) . The records of all field tests will be presented in chapter 6 together with the plots of the simulations .

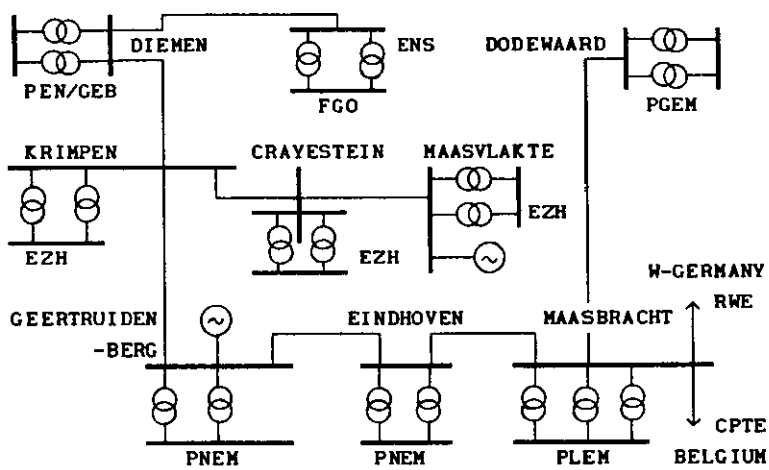

Figure 1 . Configuration of 400 kV network during the field tests

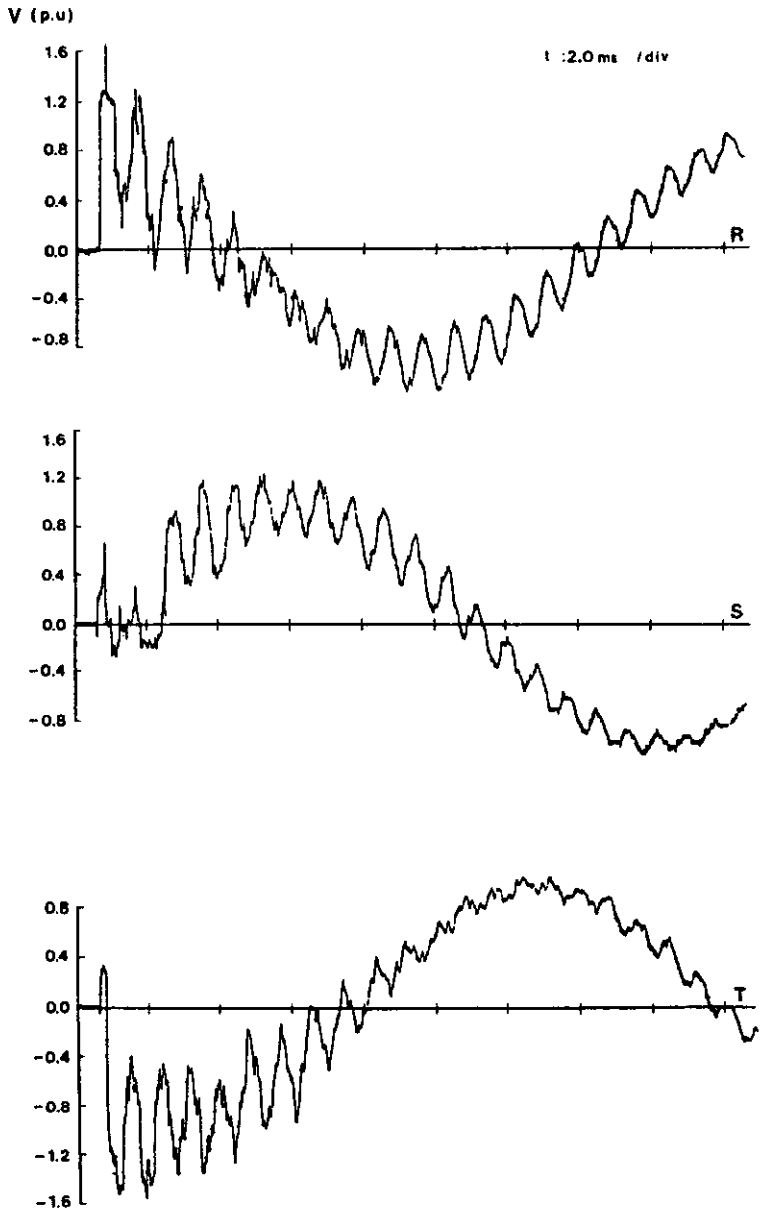

Figure 2 . Field test K6 . Receiving end overvoltages in Krimpen

test	R	S	T	test	R	S	T
K1	1.11	1.63	1.22	K9	1.56	1.58	1.34
K3	1.27	1.62	1.34	K10	1.56	1.47	1.26
K4	1.55	1.37	1.62	K11	1.57	1.58	1.30
K5	1.88	1.19	1.45	K12	1.83	1.20	1.38
K6	1.75	1.35	1.57	K13	1.60	1.09	1.38
K7	1.24	1.68	1.58	K14	1.55	1.40	1.75
K8	1.29	1.63	1.24	$\bar{X}$ =1.461p.u. σ =0.197p.u.			

Table 1 . Overvoltage peak values of field tests .

3 Network data

Whether switching transients are duplicated by analog or digital means, in both cases a large number of data is required to model the network components . It is obvious that the accuracy of any simulation method depends on the accuracy with which the various network parameters are known . In general incomplete knowledge of these parameters is the main source of error . Of major importance are :

- the positive sequence and zero sequence line parameters as a function of frequency ;
- the positive sequence and zero sequence parameters of all feeding networks ; generators , transformers , and networks of higher or lower voltage level ;
- the closing instants of the circuit breakers .

As the line parameters have been measured at power frequency , calculations of the positive sequence and zero sequence impedances as a function of frequency were necessary . For this purpose computer programs based on Carson's formula are available [14,15] . They require exact data of tower configurations and conductor arrangement . The relevant data of the 3 line types applied in the 400 kV network are given in Appendix 1 .

Data of the positive-sequence short-circuit reactances of the feeding networks were obtained from calculations of the infeeding currents in a substation due to a three phase short-circuit in that substation . Allowance was made for the generating capacity during the field test . The values of the infeeding sc-currents are given in Figure 2-1 of Appendix 2 . The short-circuit power in substation Diemen , from where the line circuit was energized , was 10.2 GVA .

The 400 kV network in its state during the field tests was feeded by several regional 150 kV networks to which most power stations were connected . Each coupling transformer consists of three single-phase three winding units . The neutrals of the star connected windings were solidly grounded in the 400 kV network whereas they were isolated in the 150 kV networks . The tertiary 50 kV windings were delta connected in order to reduce the zero-sequence short-circuit impedance. Based on the transformer data given in Appendix 2 the short-circuit reactances of each three phase unit were :

pos.-sequence $X_{1uh-h} = 57.8\ \Omega$

zero-sequence $X_{ouh} = 122\ \Omega$

In substation Ens two auto-transformers connect the 400 kV network with the northern 220 kV network whose neutrals were solidly grounded . Therefore a zero-sequence coupling between both networks exists . This has complicated the simulation of this feeding network as at first no detailed information was available on the zero-sequence impedance of the 220 kV network , as seen from substation Ens , during the field tests . A ratio of 1.2 between the zero-sequence reactance and the positive-sequence reactance at 400 kV level was assumed . Based on 3 ph-sc-current infeed of 4.3 kA , the value $X_0 = 67.5\ \Omega$ was adopted .

Triggered by the findings of Mr. Michelis (KEMA) in the EMTP simulation of field test K14 [16,17] , the representation of the feeding network in substation Ens was modified . In the EMTP calculations called EMTP-I the auto-transformers were modelled as a three winding transformer while the 220 kV network was represented by its positive-sequence and zero-sequence short-circuit impedances and surge impedances . More details are given in Appendix 2 .

In the substations Maasvlakte and Geertruidenberg generator units of 625 MVA and 500 MVA respectively were connected to the 400 kV network by means of star-delta transformers . Based on their percentage impedance voltages of 12 % and 12.9 % their zero-sequence reactances

were 32.6 Ω and 43.4 Ω respectively .

In substation Maasbracht the network was connected to the Belgian network and the W-German network by means of overhead lines . Based on information of both networks the infeeding 3 ph-sc. currents in the substation were calculated . From these data the resulting positive-sequence reactance values were determined . The zero-sequence reactances were estimated by accepting the relation $X_0 = 3\ X_1$. Table 2 summarizes the values of the sc.-reactances of the feeding networks used in the simulations . If not otherwise stated a fixed valued resistive component R = 0.1 X (50 Hz) was adopted .

substation	X_1 (Ω)	X_o (Ω)
Crayestein	1210	61
Diemen	67.2	61
Eindhoven	161.3	61
Ens	56.3	67.5 1)
Geertruidenberg	51.5	25.4
Krimpen	83.4	61
Maasbracht	7.25	13.6
Maasvlakte	80.7	21.2

1) modified at EMTP-I

Table 2. Positive-sequence and zero-sequence reactances of feeding networks at 50 Hz .

The actual instants of contact closure during the field tests were evaluated from the voltage records . They are given in Table 2-1 of Appendix 2 .

4 Calculations by EMTP

The ElectroMagnetic Transient Program (EMTP) is a general purpose computer program for simulating fast transients in electric power systems . For 15 years the Bonneville Power Administration (Portland, Oregon) and others have developed the program and distributed it worldwide [18] . In Europe users have formed the European Users Group with a coordination center at K.U. Leuven (Belgium) [1)]. The program features a wide variety and range of modelling capabilities used to model electromagnetic and electromechanical transients . Included are the modelling of travelling waves on overhead lines and cables , lumped linear elements , transformers , synchronous machines etc. , as further documented in Ref . [14] .

In general a network consists of several substations interconnected by lines and of infeeds from power plants or from other networks, directly or via transformers . A detailed representation of all components will result in large computation times and memory requirements . So , for practical reasons some form of network reduction is necessary . In the EMTP duplication of the field tests all transmission lines of the network as shown in Figure 1 were represented by distributed parameter elements with the exception of the lines Maasbracht-Dodewaard , Maasbracht-Belgium and Maasbracht-W.Germany . No attempts were made to reduce the simulated network further as it was not the aim of the EMTP calculations to investigate the permissible network reduction .

4.1 Representation of transmission lines

In EMTP a number of line models are available ranging from single-phase, lossless and distortionless models up to multi-phase, frequency-dependent , untransposed line models . In this study the most advanced model [J.Marti] was used [19] . This model accounts for the frequency dependence of the line parameters . Due to the electromagnetic coupling

1) K.U. LEUVEN EMTP CENTER
KARD. MERCIERLAAN 94
B-3030 HEVERLEE-BELGIUM

between the overhead conductors the travelling waves are also coupled . Decoupling of these travelling waves by means of modal decomposition is a generally applied technique . A proper selection of the transformation from phase quantities to modal quantities , will result in a set of independent travelling wave components called " modes " . As in EMTP all calculations are performed in the time domain , the transformation matrices should be real and frequency independent . This is the case for balanced line configurations . In case of transposed double circuit lines the errors due to the assumption of constant transformation matrices will be very small . Within certain frequency limits this assumption is even acceptable for untransposed lines [20] .

Except for the triple-circuit line Geertruidenberg-Eindhoven all lines are double-circuit lines where each circuit was transposed at two intermediate points . Normally the circuits are in parallel operation . So all lines , except the switched line , were modelled as balanced three-phase lines . The wave propagation is characterized by a ground mode and two identical aerial modes . The switched line Diemen-Krimpen was modelled as six-phase line with two balanced circuits . Its wave propagation is characterized by a ground mode , an interline mode and four identical aerial modes . Additional information regarding the " JMarti-setup " is given in Appendix 1 .

4.2 Representation of feeding networks

As stated before all 400 kV lines were represented in detail with the exception of some lines connected to substation Maasbracht . So all infeeds to represent were transformer infeeds with the exception of substation Maasbracht . Each was modelled by a three-phase e.m.f. in series with a three-phase coupled R-L network as shown in Figure 3 .

The values of R and L 's were based on the positive-sequence and zero-sequence impedances at power frequency as given in Table 2 .

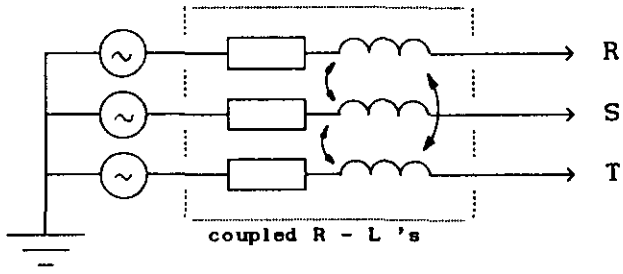

Figure 3 Model of transformer infeed .

In substation Maasbracht the transformer infeeds and the infeeds from the lines not represented in detail , were combined and represented like the pure transformer infeeds described above . However , to account for the initial reflections , the resulting positive-sequence and zero-sequence surge impedances of the three lines in parallel were incorporated in the model of Figure 3 . This was realised by adding resistive branches parallel to the R-L branches . (R_1=52.5 Ω, R_0=153.3 Ω)

The feeding network in substation Ens was modelled in two different ways . In the calculations called EMTP-II the network was modelled according to Figure 3 . In the calculations called EMTP-I the auto-transformers were modelled as three single-phase three-winding transformers with 1 : 1 turn ratios . The 220 kV network behind the transformer was represented similarly to the network termination in substation Maasbracht . Figure 4 shows the equivalent network applied .

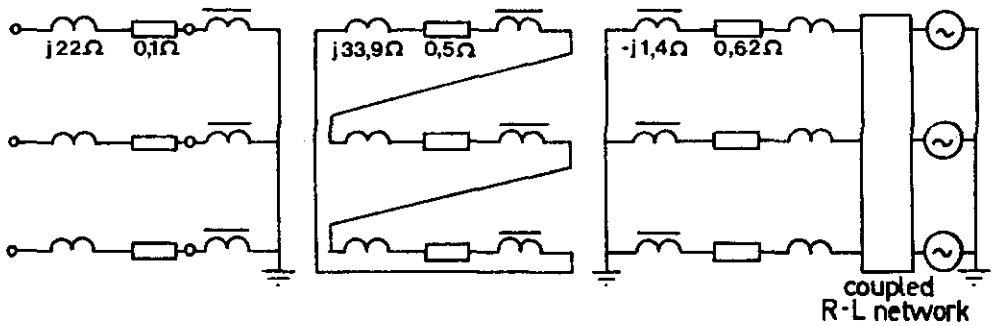

Figure 4 Equivalent feeding network in Ens

The data for the coupled R-L and surge-impedance network are given in Appendix 2 . The capacitances and inductances of measuring transformers and busbars were not taken into account .

4.3 Calculation results

The calculations were carried out with EMTP version M39 . A time-step of 5 μs was chosen and the receiving-end overvoltages were calculated over 20 ms . The switching moments evaluated from the field test records were applied .

Results of EMTP-II

Figure 5 shows calculated receiving-end overvoltages corresponding to test K6 .

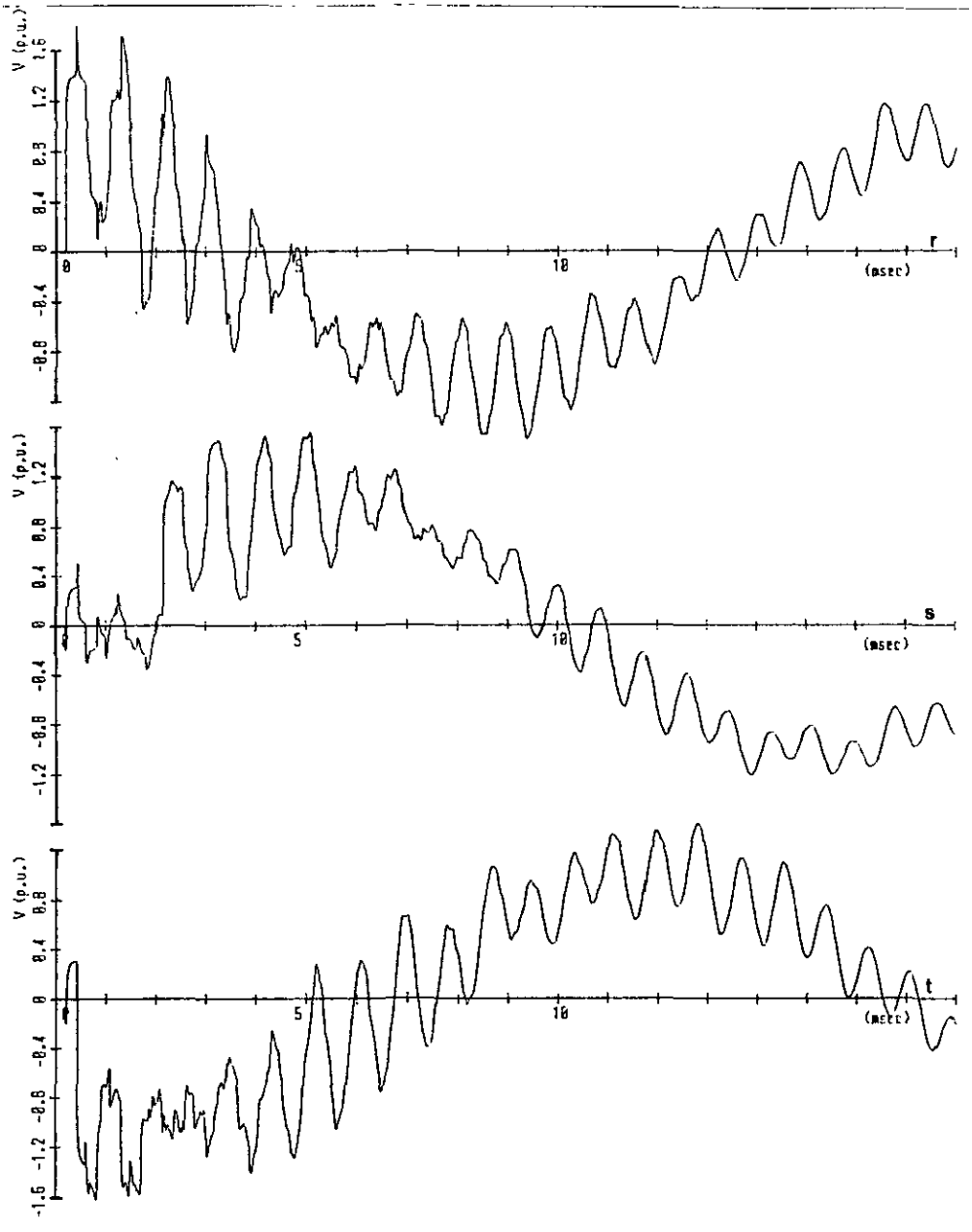

Figure 5 . EMTP-II test K6 . Receiving-end overvoltages in Krimpen

The maximum overvoltage in phase R is somewhat higher than measured in the field test ; 1.82 p.u. versus 1.75 p.u. . The plots of the other tests will be presented and discussed in chapter 6 . The overvoltage peak values of all line-energizations have been listed in Table 3 . The mean value of 1.632 p.u. is about 12 % higher than the mean value derived from the field tests .The standard deviations are nearly equal.

test	R	S	T	test	R	S	T
K1	1.32	1.64	1.63	K9	1.72	1.68	1.25
K3	1.51	1.69	1.56	K10	1.88	1.56	1.64
K4	1.56	1.48	2.15	K11	1.77	1.64	1.27
K5	1.96	1.43	1.72	K12	1.95	1.28	1.75
K6	1.82	1.57	1.63	K13	1.71	1.48	1.83
K7	1.50	1.86	1.65	K14	1.56	1.71	1.77
K8	1.37	1.61	1.56	$\bar{X}$ =1.632p.u.		σ =0.194p.u.	

Table 3 Overvoltage peak values of EMTP-II calculations

Comparing Figure 5 with Figure 2 shows that the shape of the waveforms corresponds fairly well , especially during the first milliseconds . However in the calculated waveforms the predominant oscillations have higher initial amplitudes and are less damped . On the other hand the high-frequency irregularities , clearly observable in the field test waveforms , are only present during the first milliseconds . Since all 400 kV lines were represented by frequency dependent line models the differences between measured and calculated waveforms must be related to the representation of the transformer infeeds . Triggered by findings of KEMA 's study [16] , the representation of the feeding network in substation Ens was modified as described in the previous chapter .

Results of EMTP-I

After the modification the calculations were repeated . The calculated voltage waveforms corresponding to test K6 have been plotted in Figure 6 .

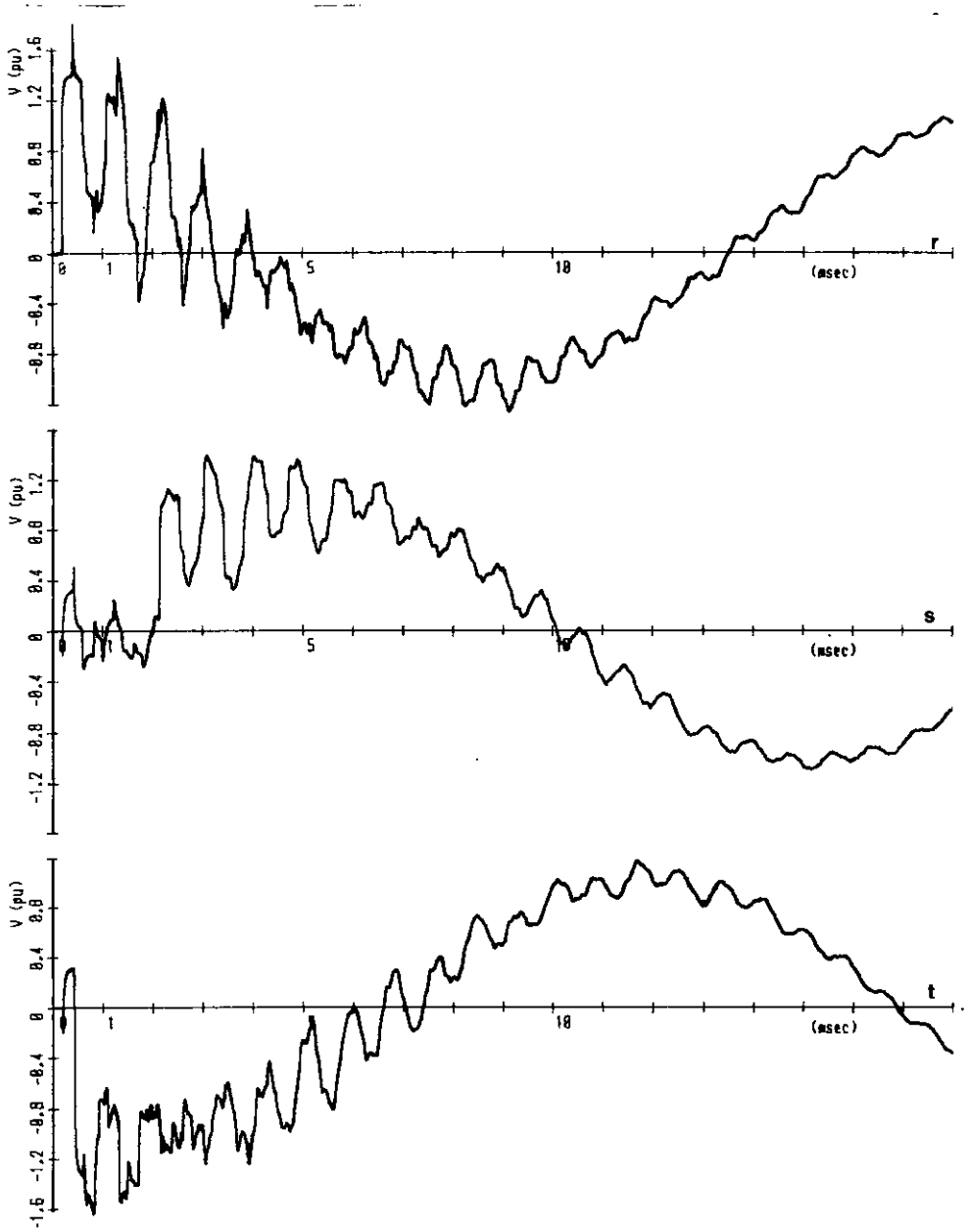

Figure 6 . EMTP-I test K6 . Receiving-end overvoltages in Krimpen

Comparing this figure with Figure 2 , it can be observed that the resemblance is quite good over the whole time span . The surge-impedance modelling of the 220 kV lines in substation Ens has increased the damping of the predominant oscillations . Whether it has also affected the high frequency irregularities is difficult to conclude , however in Figure 6 they are more pronounced than in Figure 5 .

The overvoltage peak values of all line-energizations have been listed in Table 4 . The difference between their mean value and the mean value of the measured overvoltage peaks is within 5 % . The Gaussian standard deviation is about 14 % higher .

test	R	S	T	test	R	S	T
K1	1.17	1.64	1.34	K9	1.50	1.65	1.19
K3	1.36	1.55	1.32	K10	1.67	1.35	1.48
K4	1.56	1.35	2.01	K11	1.67	1.62	1.17
K5	1.91	1.25	1.66	K12	1.97	1.17	1.67
K6	1.81	1.40	1.64	K13	1.66	1.26	1.65
K7	1.29	1.87	1.65	K14	1.56	1.54	1.78
K8	1.34	1.61	1.41	$\bar{X}$ =1.531p.u.		σ =0.224p.u.	

Table 4 . Overvoltage peak values of EMTP-I calculations

5 Simulation on TNA

The original version of the transient network analyzer, manufactured by Reyrolle Ltd , was installed in 1978 [21] . Later on new double-circuit line models were designed and existing line models were improved . The manually controlled switches were replaced by computer controlled electronic switches . They provide automatic statistical analyses with control of prestrike characteristics and mechanical closing moments . The measuring system consists of several A/D converters and a 6 channels peak-voltage detector , all interfaced with the process computer . Figure 7 shows the block diagram .

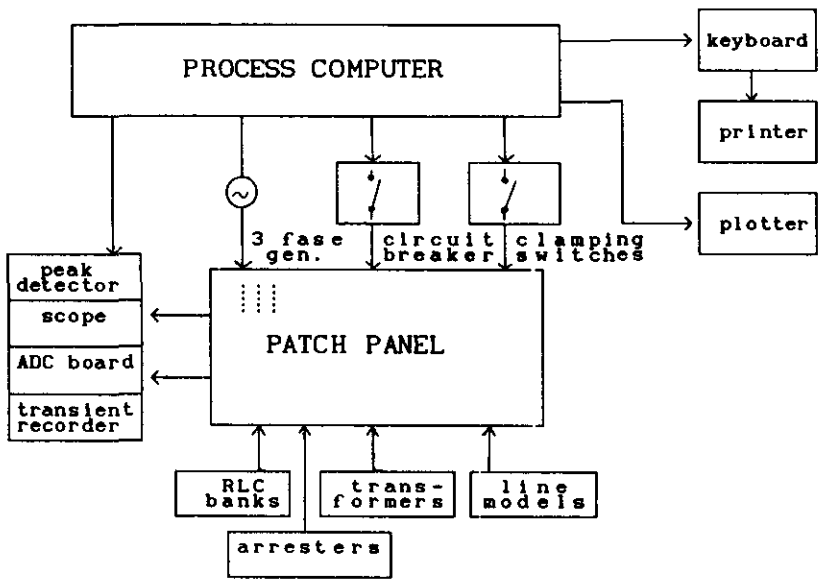

Figure 7 . Block diagram of TNA

The operating frequency of the generators is continuously variable over the range 40 Hz - 500 Hz , allowing frequency scaling to be employed . The repetition rate is adjustable between 1 - 99 cycles of the operating frequency , while switching moments can be adjusted in steps of one degree. The phase voltages are variable up to 10 V rms .As voltages and currents are scaled-down in the same rate , impedances are not scaled .

5.1 Transmission line model

In the duplication of the field tests the 57.7 km long double-circuit transmission line Diemen-Krimpen was modelled by a series-connection of 20 Π -sections . With the TNA operating on a basic frequency of 96 Hz , each Π -section was equivalent to 2.88 km . The diagram of a double-circuit Π -section is shown in Figure 8 .

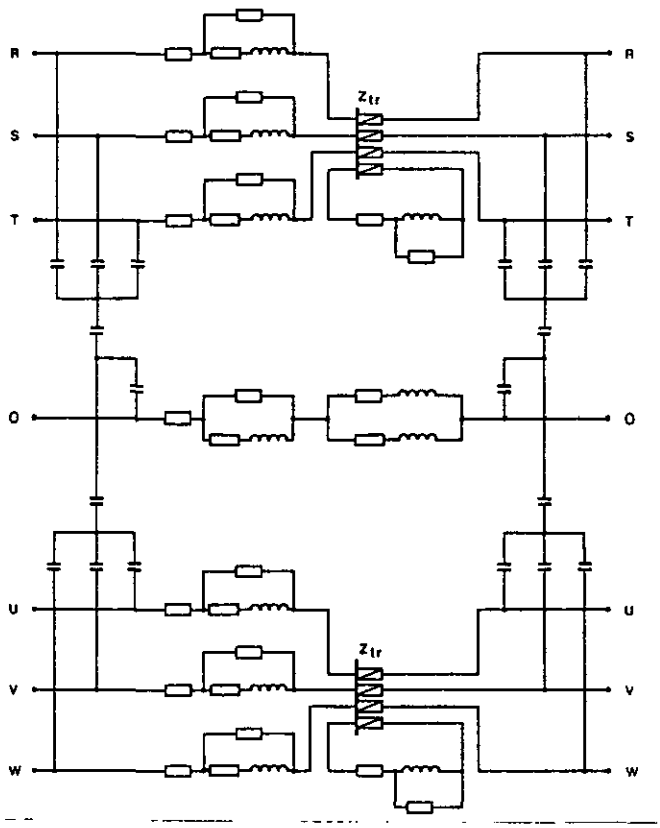

Figure 8 . Double-circuit Π -section

The Π -sections were constructed with fixed inductors to meet the high quality factor of the 400 kV line . Much effort was devoted in modelling the frequency dependent inductances and resistances of line conductors and ground-return . After the construction the impedances

versus frequency of all branches were measured . With these data the wave propagation characteristics of a Π -section , being part of a tandem of many sections , were calculated and related to those calculated for the relevant line . The percentage deviations of the positive , the intercircuit , and the zero-sequence propagation characteristics versus frequency are given in Figure 3-1 of Appendix 3. The tolerance limits specified by Cigré WG 13.05 [3] were satisfied in the frequency range up to 10 kHz .

It is well known that the step response of a finite number of Π-sections comprises spurious oscillations of high frequency resulting in an overshoot of some 20 % . These oscillations were reduced by connecting resistors of 2K7 Ω across the inductors representing the positive-sequence line inductance . By this measure the overshoot in the step response was limited to 6 % . The additional damping resistors reduced the frequency bandwidth of the line model in a certain extent .

5.2 Feeding network model

Due to the limited number of Π -sections available it was impossible to model all lines in detail as in EMTP . So only the line Diemen-Krimpen was modelled by Π -sections while the partial networks on both sides of this line were modelled by means of equivalent circuits as shown in Figure 9 . The application of a decoupling transformer allowed the separate modelling of the positive-sequence impedances and the zero-sequence impedance . The circuits indicated by Z_1 and Z_0 represented the positive-sequence and zero-sequence driving point impedances respectively of the partial network as seen from either substation Diemen or substation Krimpen . Dimensioning of these so-called Foster circuits required knowledge of the zero-sequence and positive-sequence impedances of the actual networks over a frequency range up to several kilohertz . These calculations were based on the following data and presuppositions :

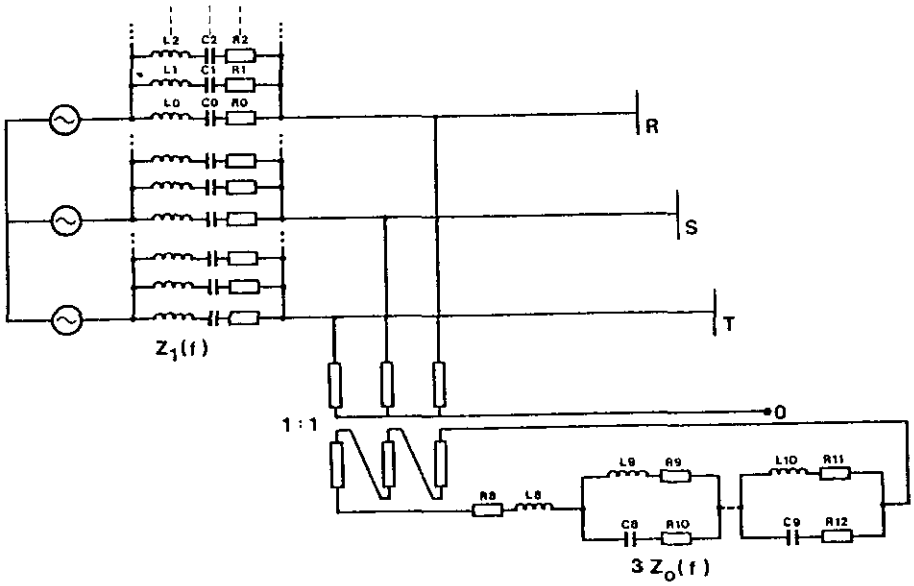

Figure 9 . Feeding network equivalent circuit

- the network configuration during the field test as given in Figure 2-1 of Appendix 2 .
- the distributed series impedances and shunt admittances versus frequency of each 400 kV line .
- the positive-sequence and zero-sequence impedances versus frequency of all infeeds in the 400 kV substations . It was assumed that each impedance could be represented by an L - R series circuit . The values of the inductances were based on the 50 Hz sc-reactances as given in Table 2 , while the values of the resistances were kept constant ; R = 0.1 X (50 Hz).

With these data the admittance matrices of the positive-sequence network and of the zero-sequence network were calculated for a large number of discrete frequencies in the range of interest . By means of ordering and Gauss-elimination the driving point impedances of the partial networks were obtained . Figure 3-2 of Appendix 3 shows the calculated impedances versus frequency of the partial network terminating in sub-station Krimpen while Figure 3-3 applies to the partial network Diemen . These figures clearly illustrate the complex

nature of the networks with a number of series and parallel resonances . Z_1 (f) and Z_0 (f) can be synthesized by adopting a rational lossless impedance or admittance function and applying partial fraction expansion (Foster and Cauer synthesis) [22] .

An equivalent network with identical characteristics can be constructed by either a parallel arrangement of series-resonance L - C circuits (Foster II) or a series arrangement of parallel L - C circuits (Foster I) . The number of resonance circuits equals the number of series or parallel-resonance frequencies of Z (f) in the frequency range of interest . A computer program was developed to calculate the L and C values of the equivalent Foster circuits based on the frequencies of poles and zeros and the 50 Hz impedance as listed in Appendix 3 .

The positive-sequence impedances were simulated by Foster II circuits . Foster I circuits were applied in the simulation of the zero-sequence impedances allowing correction for the transformer reactance . After construction some resistors were added to adapt the resistive values at resonance frequencies . In Figure 3-2 and Figure 3-3 the impedances of the realised equivalent circuits have been plotted . These plots have been corrected for the frequency transformation applied on the TNA. The number of resonance circuits was selected to match the frequency dependent impedances up to 3.2 kHz . This corresponded with 2.5 times the fundamental frequency of the switched line . Above the last zero modelled , the equivalent circuits behave inductive . Attemps to adapt the high frequency characteristics to the surge impedances of the lines failed as this affected too much the quality of poles and zeros in the upper part of the frequency range .

The voltage sources of both feeding networks were adjusted in-phase , so no power was flowing through the interconnecting line .

5.3 Simulation results

One circuit of the line model was energized from feeding network Diemen by means of Power-Mosfet electronic switches . The switching moments were as listed in Table 2-1 . Before each switching operation the line circuit was discharged . The receiving-end overvoltages were registered by 10 bits transient recorders with a sample frequency of 200 kHz . Simultaneously the peak values were measured by fast sampling and hold circuits and stored in memory . Figure 10 shows the measured receiving-end voltages corresponding to test K6 . The plots of the other tests will be presented and discussed in chapter 6 . The overvoltage peak values of all line-energizations have been listed Table 5 . Their mean value is 1.487 p.u. and the standard deviation is 0.215 p.u. .

test	R	S	T	test	R	S	T
K1	1.215	1.565	1.365	K9	1.585	1.54	1.04
K3	1.475	1.66	1.265	K10	1.625	1.34	1.565
K4	1.480	1.255	2.035	K11	1.67	1.565	1.075
K5	1.62	1.165	1.475	K12	1.68	1.095	1.505
K6	1.74	1.555	1.615	K13	1.68	1.245	1.775
K7	1.345	1.69	1.47	K14	1.31	1.67	1.705
K8	1.325	1.635	1.375	$\bar{X}$ =1.487p.u.		σ =0.215p.u.	

Table 5 . Overvoltage peak values of TNA simulations

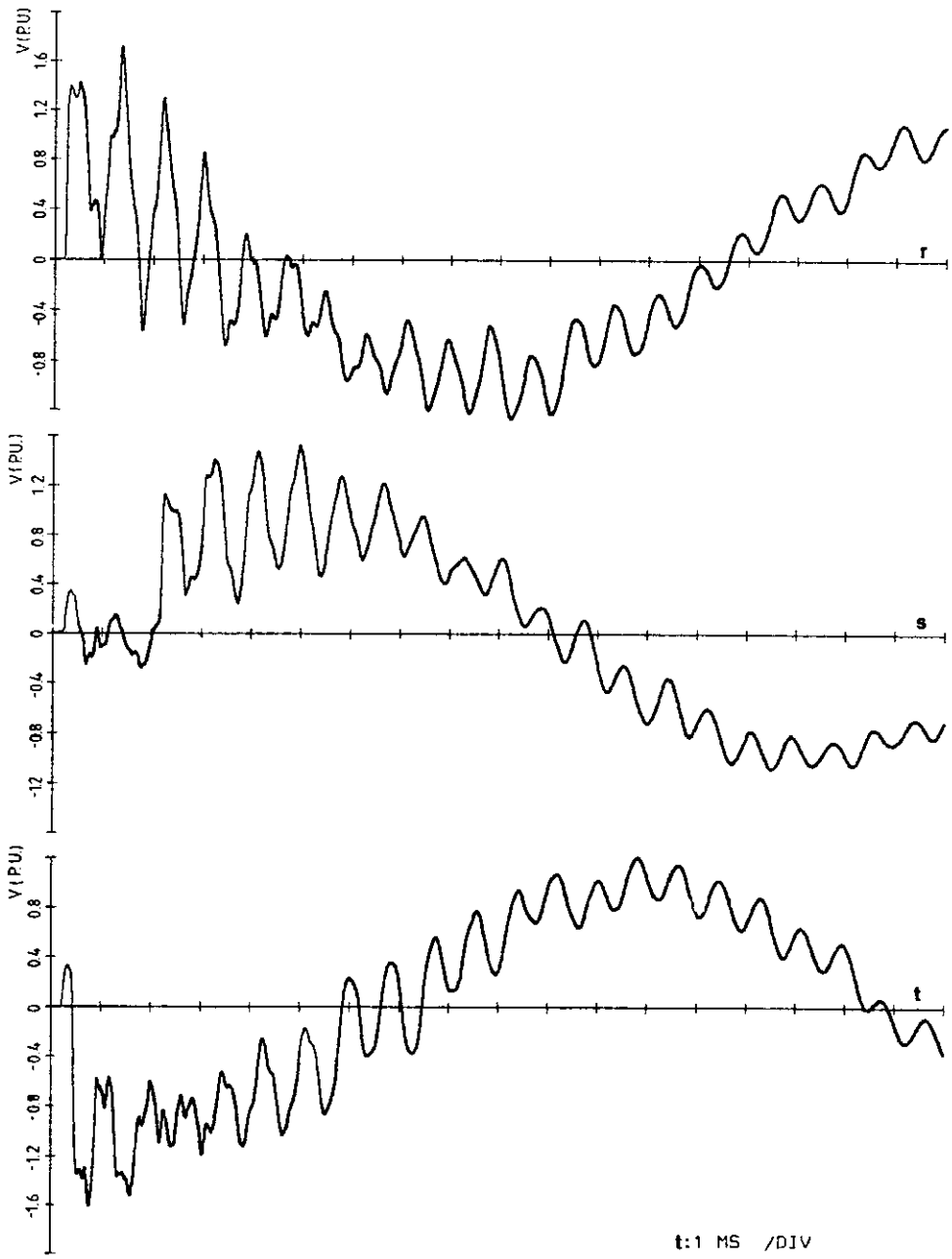

Figure 10 . TNA *simulation of test* K6 .
Receiving-end overvoltages in Krimpen

6 Comparison of results

The waveforms of the receiving-end phase-to-ground voltages recorded during the field tests and the corresponding waveforms from the simulations by EMTP and TNA are shown in Figure 11 through 23 . They have been grouped for each test for the sake of comparison . The waveforms of all simulations have been plotted for a time span of 18 ms in order to show both the initial transients and the predominant oscillations . Most field records presented have a time window of 5 ms. Field records over several 50 Hz cycles are available and have been used in determining the overvoltage peak values but these UV-records are unsuitable for reproduction .

A good resemblance of the waveforms during the first milliseconds after contact closing may be observed for instance in Figure 17 by comparing the waveforms calculated by EMTP and the record of field test K8 . This indicates the correct simulation of the network in the time span where multiple reflections determine the voltage shape . In some figures a poorer resemblance can be observed after the closing of the third pole of the circuit-breaker . This can be attributed to the difficulty in estimating the exact time delay between the first and the third pole closing in those tests where the voltage jump due to third pole closing was relative small . This applies to the tests K3,K4,K5,K7,K9,K11 and K13 . Besides differences in time delays also the switching moments of the first closing pole applied in the simulations may have some deviations because they were determined from UV-records with a time scale of 0.4 ms/cm . The estimated switching moments have been marked in the field records by asterisks . It may be expected that slight modifications of the closing moments could have improved the resemblance of the waveforms .

Of all simulations the results of EMTP-I show the best resemblance to the field tests . During the first milliseconds the waveforms of the EMTP-II simulations are identical to those of EMTP-I .

Figure 11 . Receiving-end overvoltages in Krimpen of test K 1

KEMA field test

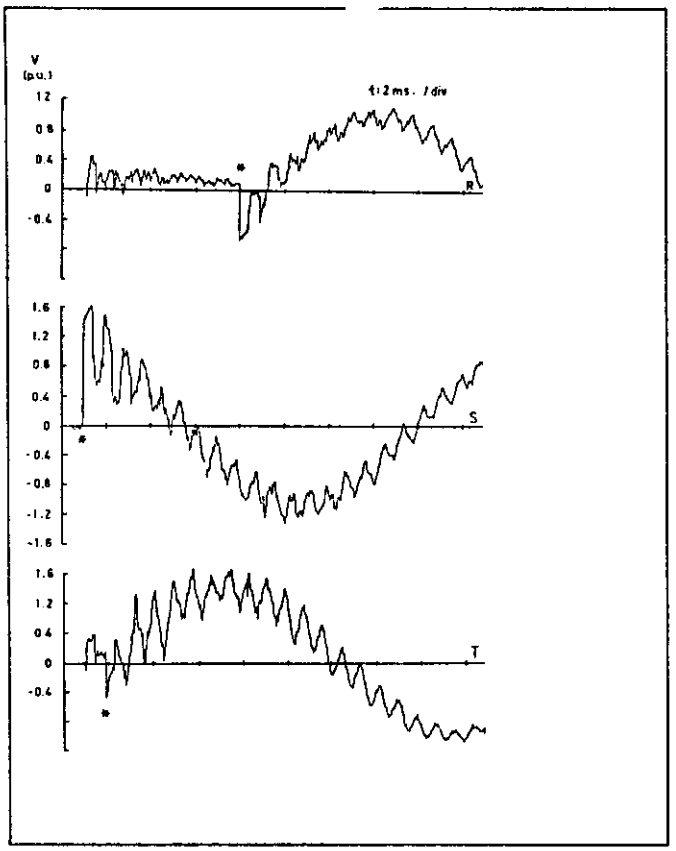

TNA Simulation

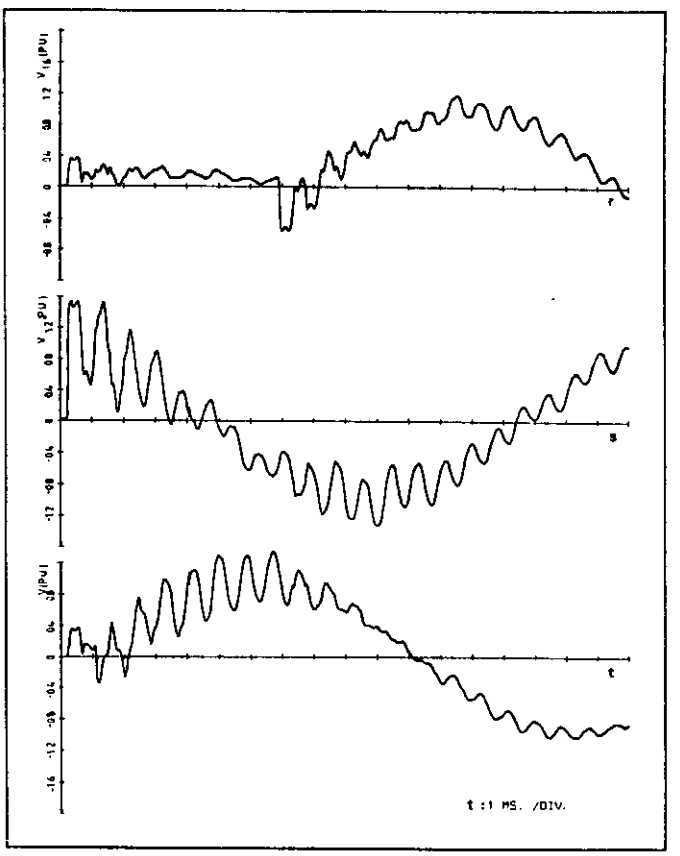

EMTP-I Calculations

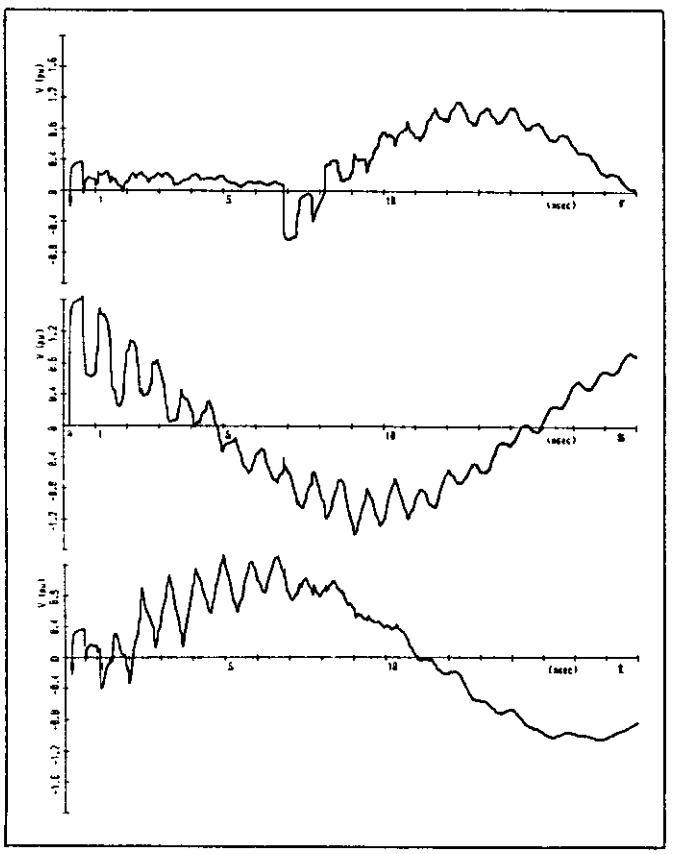

EMTP-IICalculations

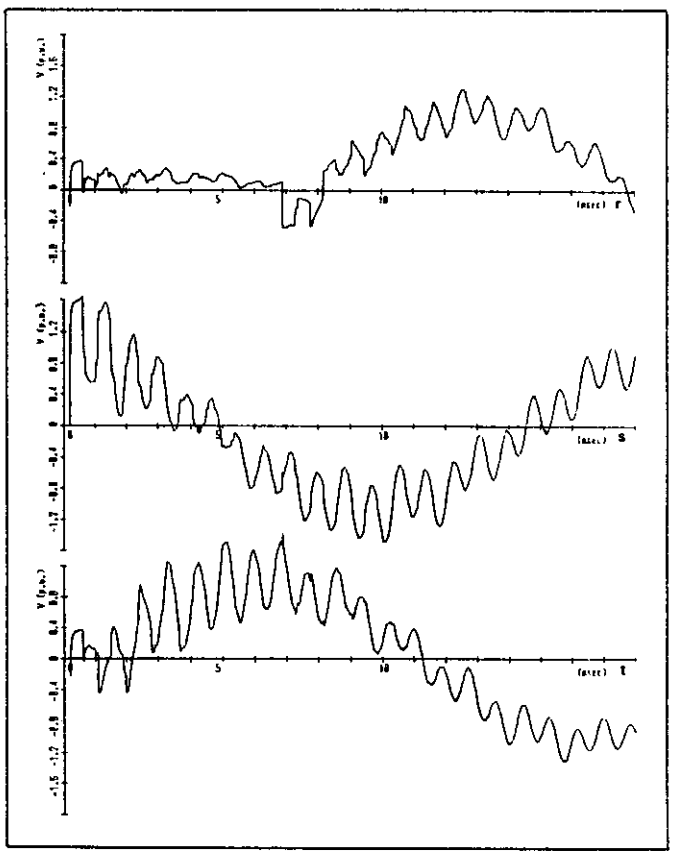

Figure 12 . Receiving-end overvoltages in Krimpen of test K 3

KEMA field test

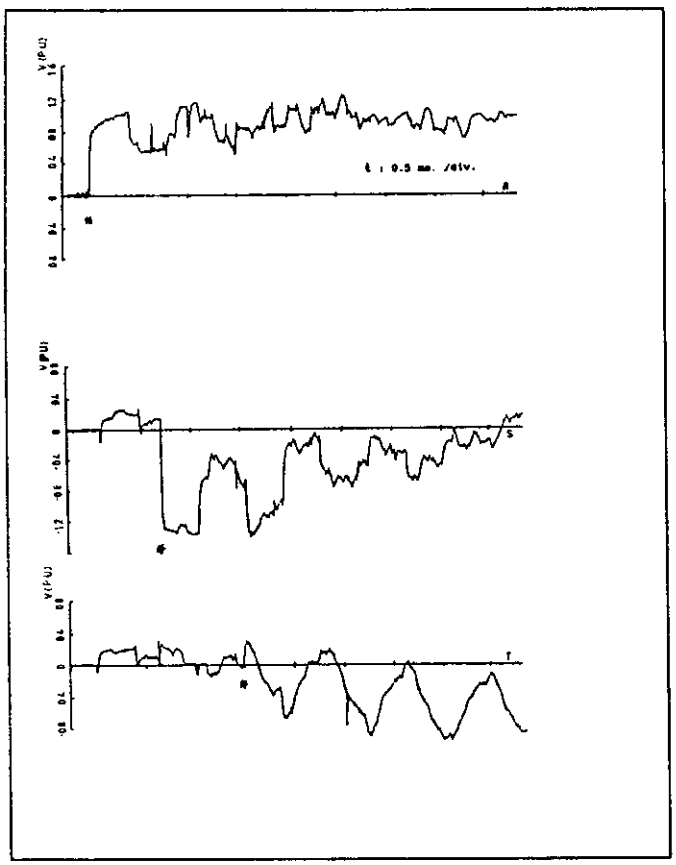

TNA Simulation

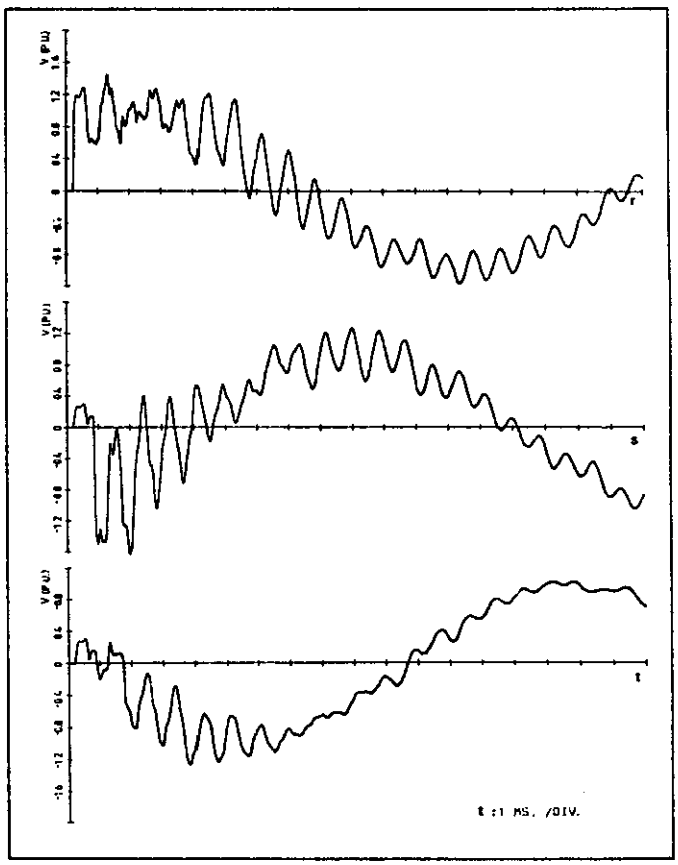

EMTP-I Calculations

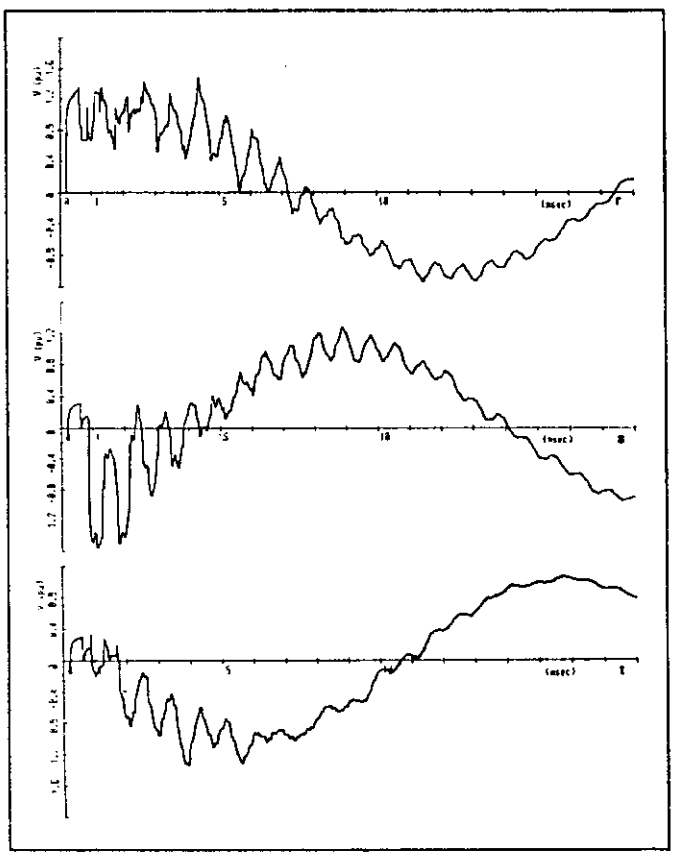

EMTP-II Calculations

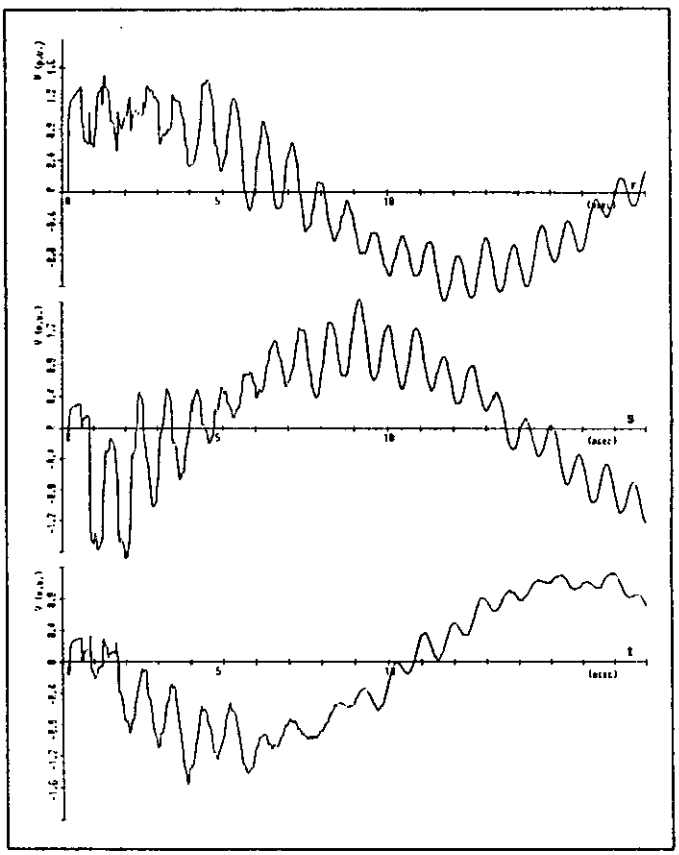

Figure 13 . Receiving-end overvoltages in Krimpen of test K 4

KEMA field test

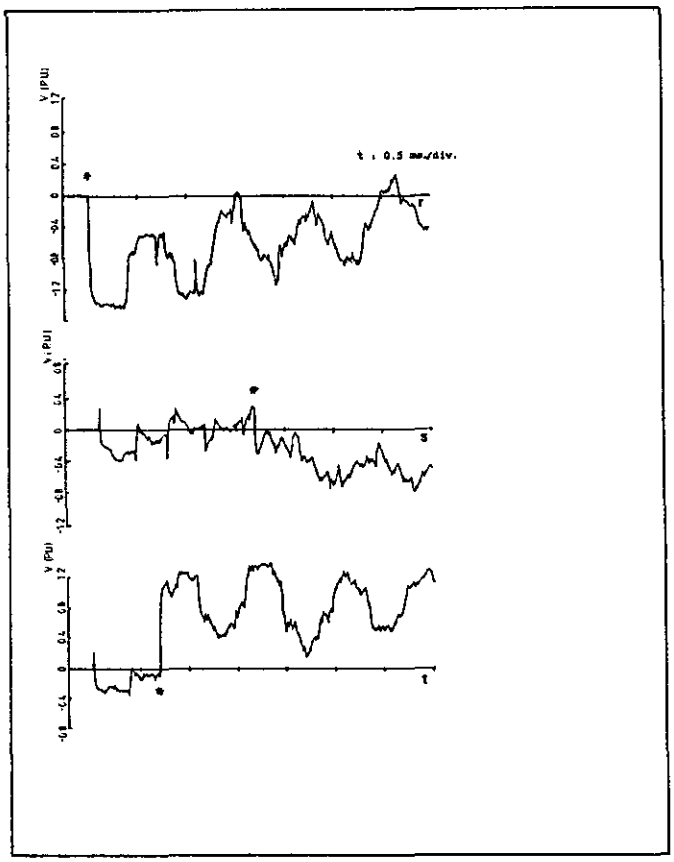

TNA Simulation

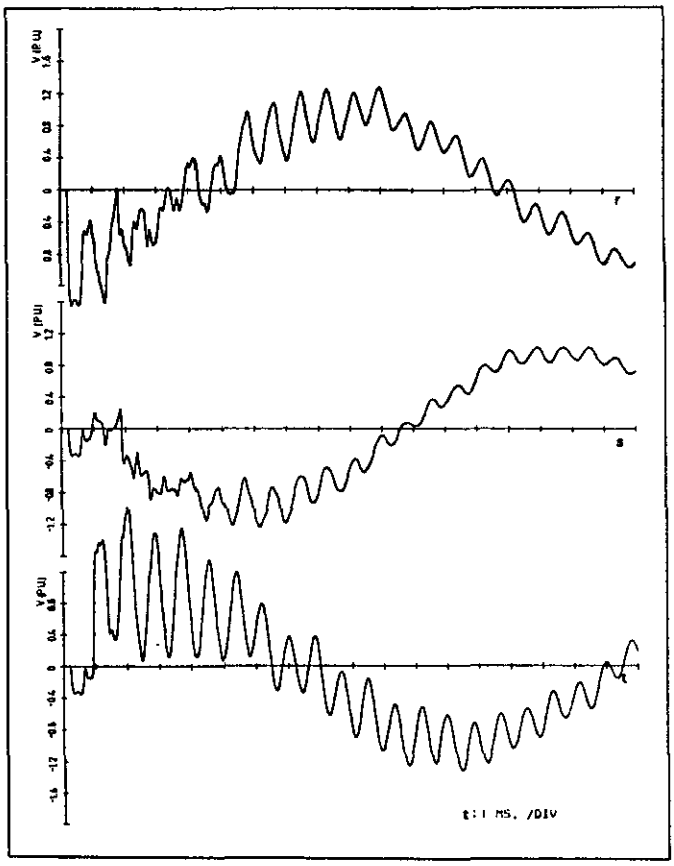

EMTP-I Calculations

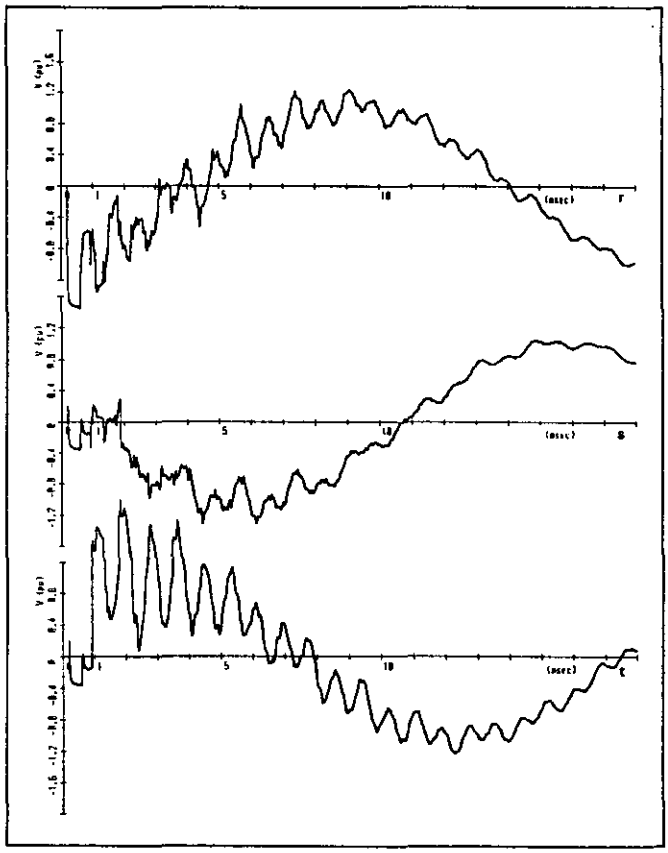

EMTP-II Calculations

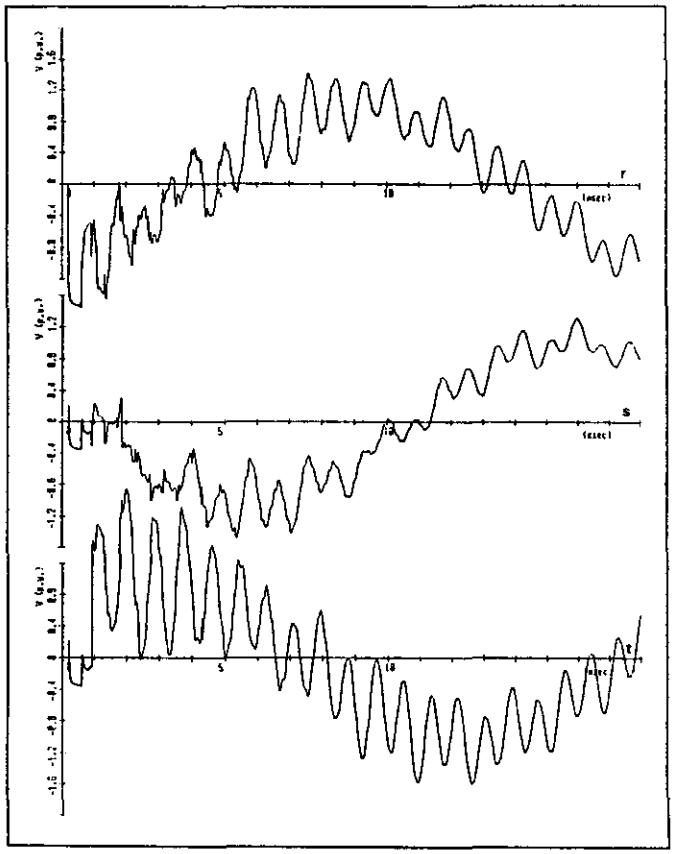

Figure 14 . Receiving-end overvoltages in Krimpen of test K 5

KEMA field test

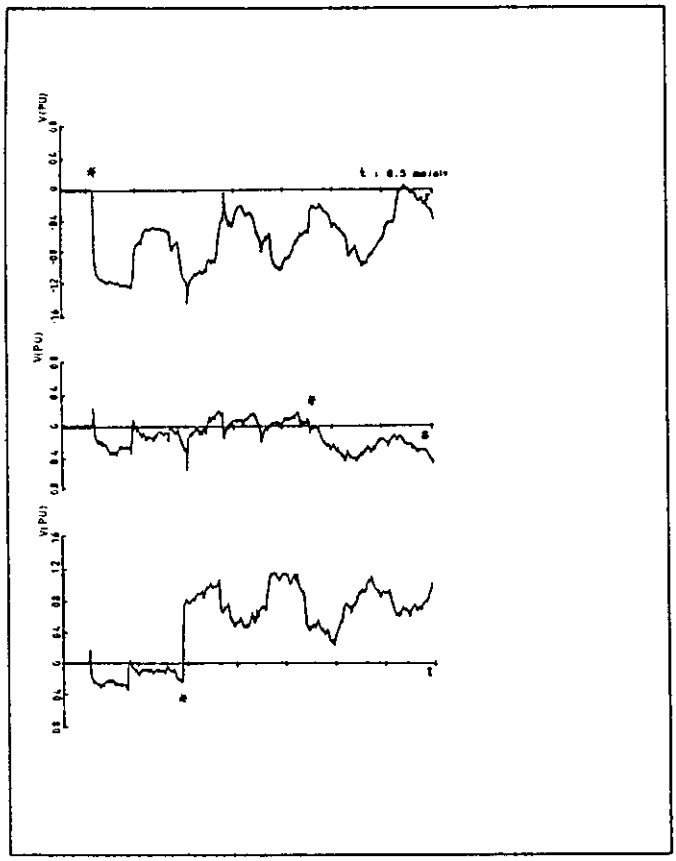

TNA Simulation

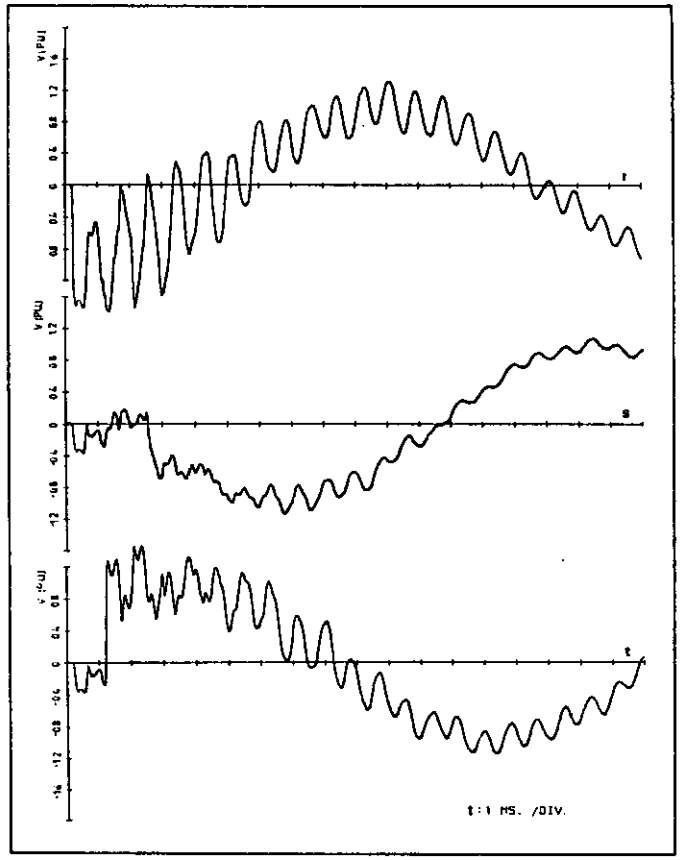

EMTP-I Calculations

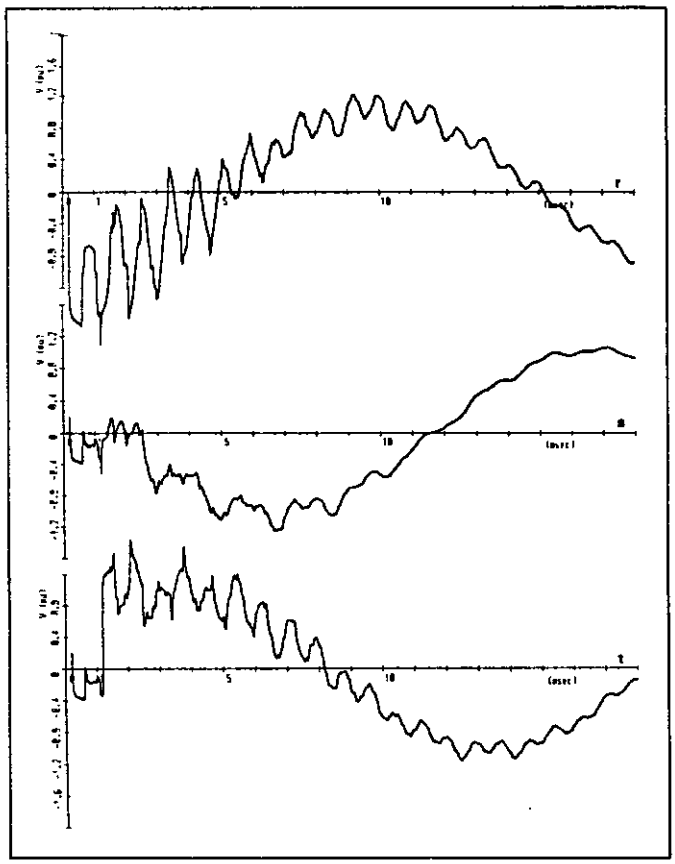

EMTP-II Calculations

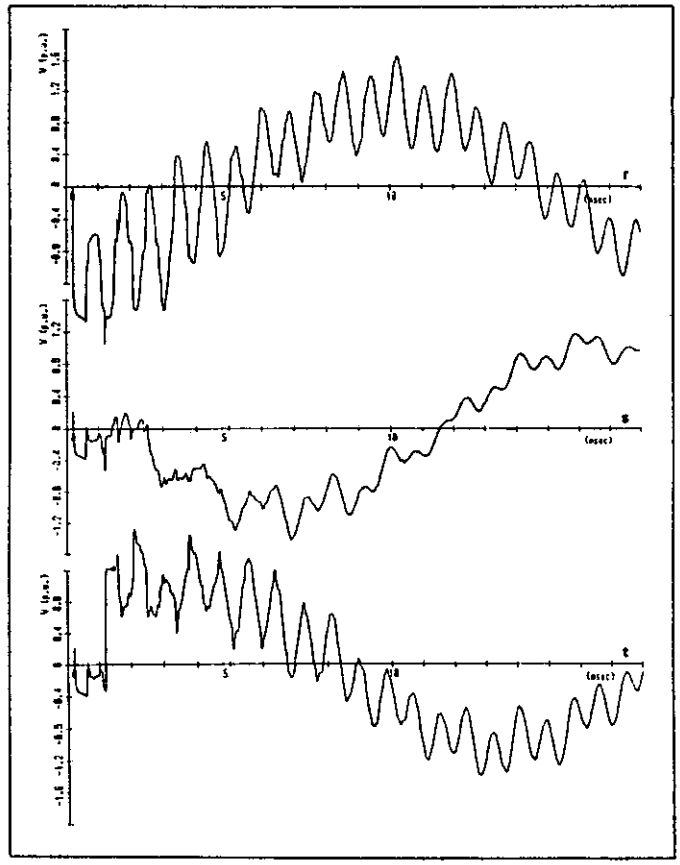

Figure 15 . Receiving-end overvoltages in Krimpen of test K 6

KEMA field test

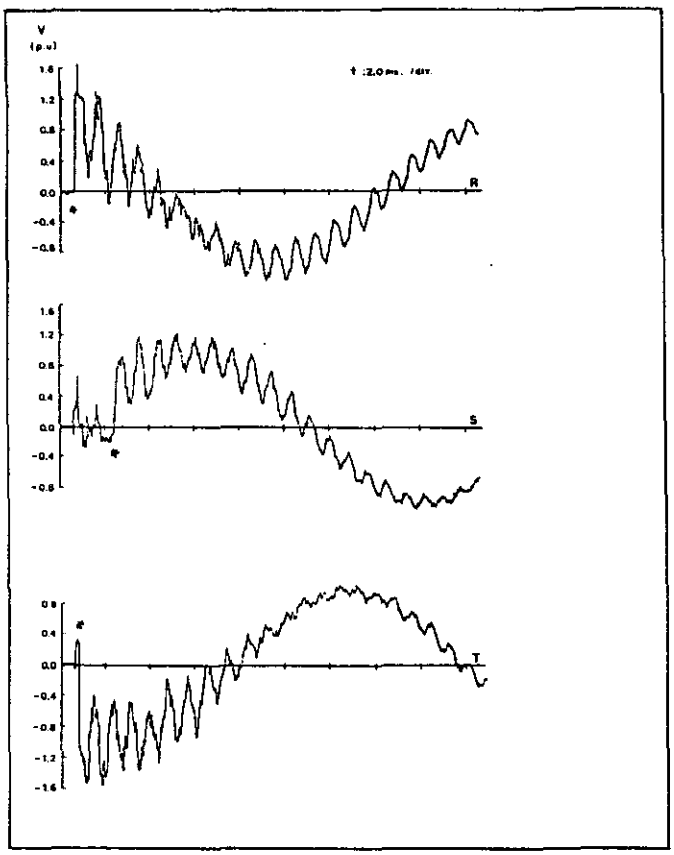

TNA Simulation

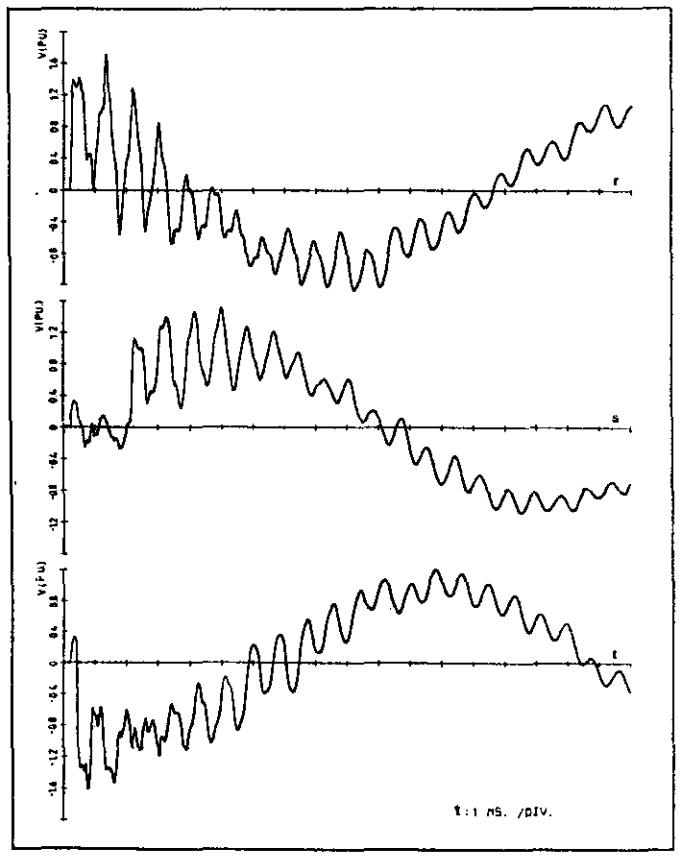

EMTP-I Calculations

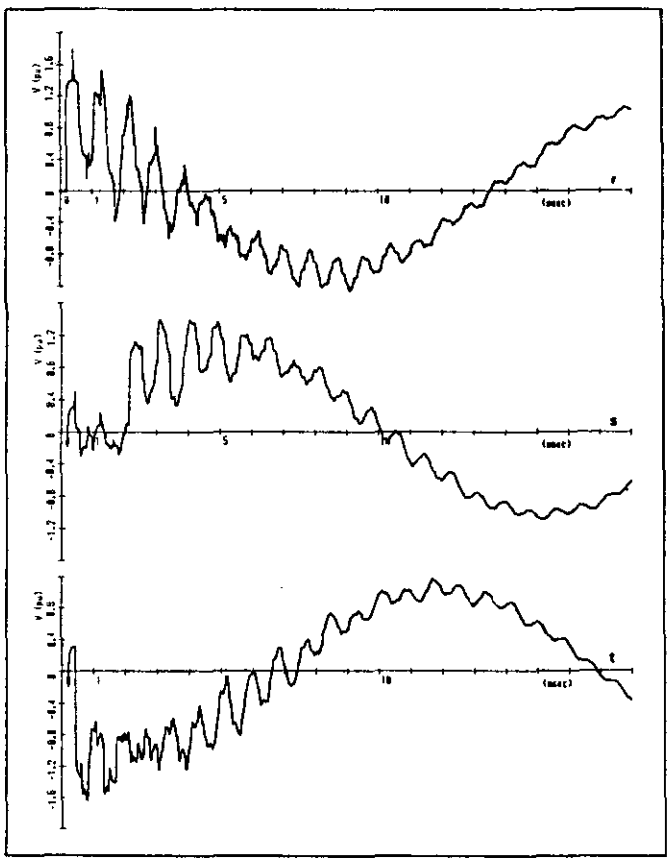

EMTP-IICalculations

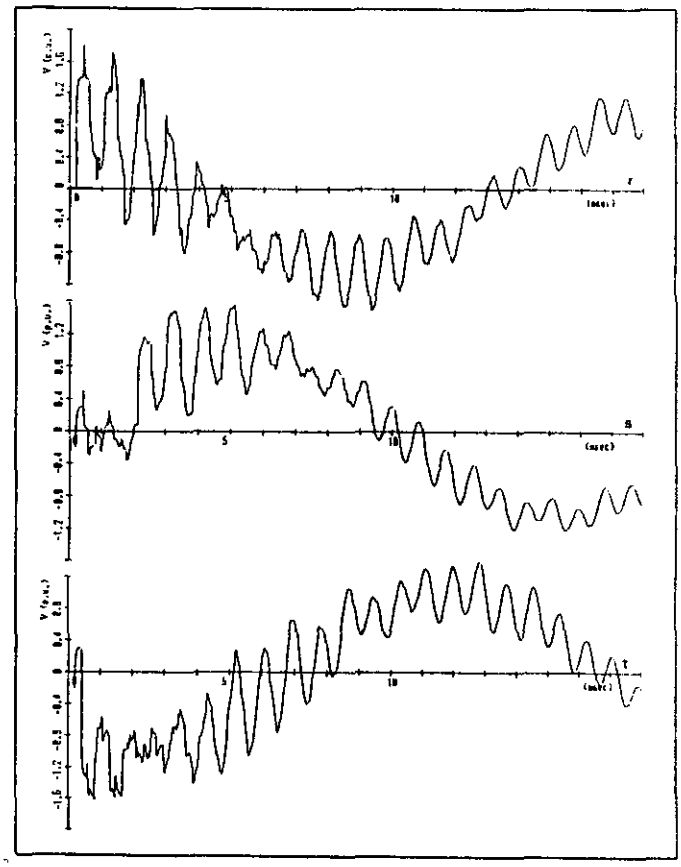

Figure 16 . Receiving-end overvoltages in Krimpen of test K 7

KEMA field test

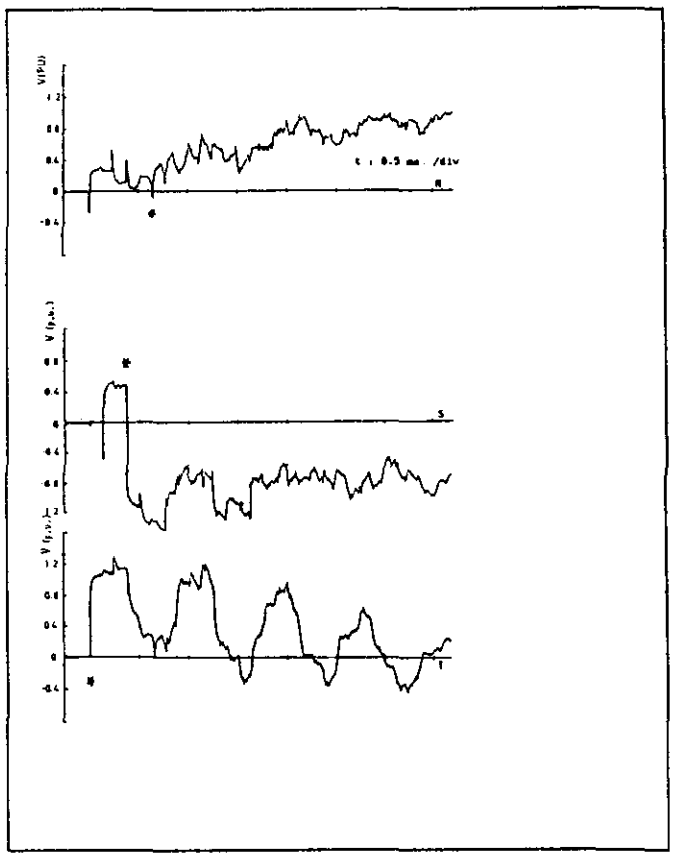

TNA Simulation

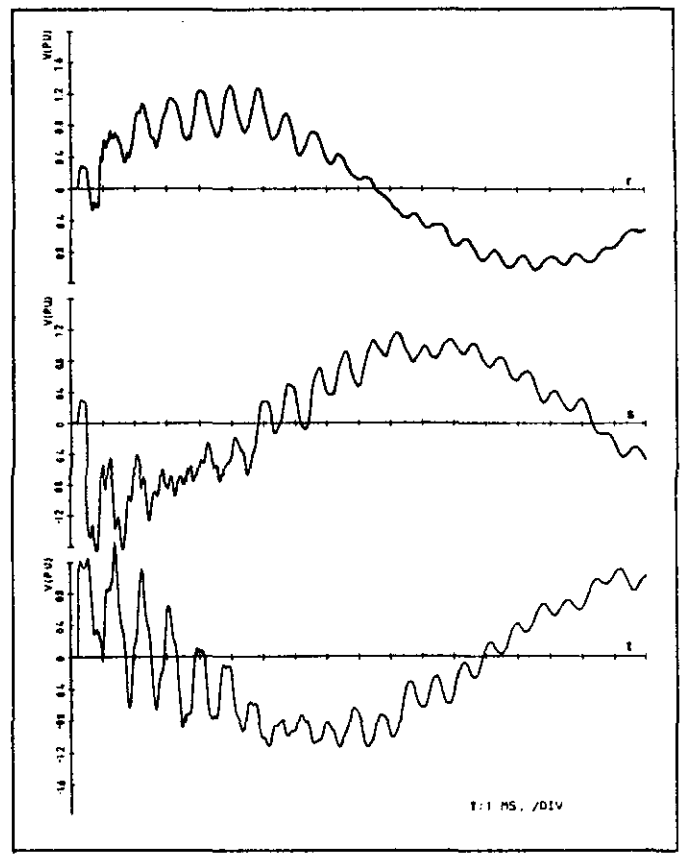

EMTP-I Calculations

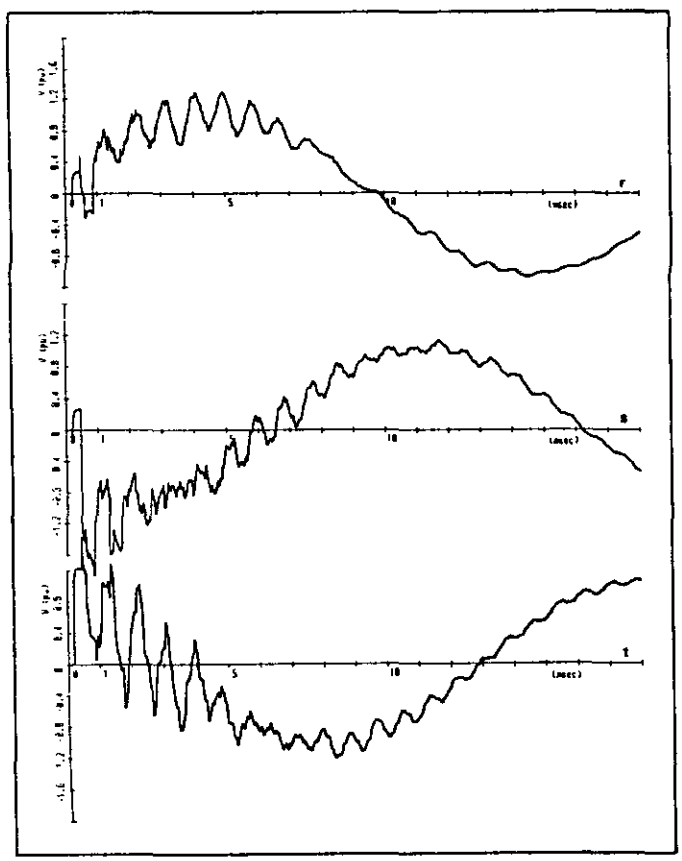

EMTP-II Calculations

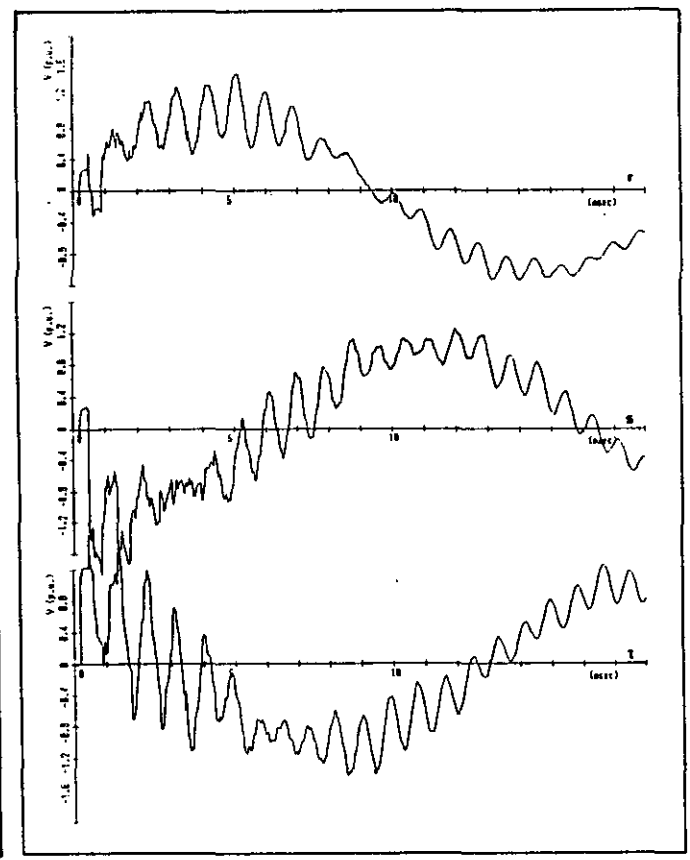

Figure 17 . Receiving-end overvoltages in Krimpen of test K 8

KEMA field test

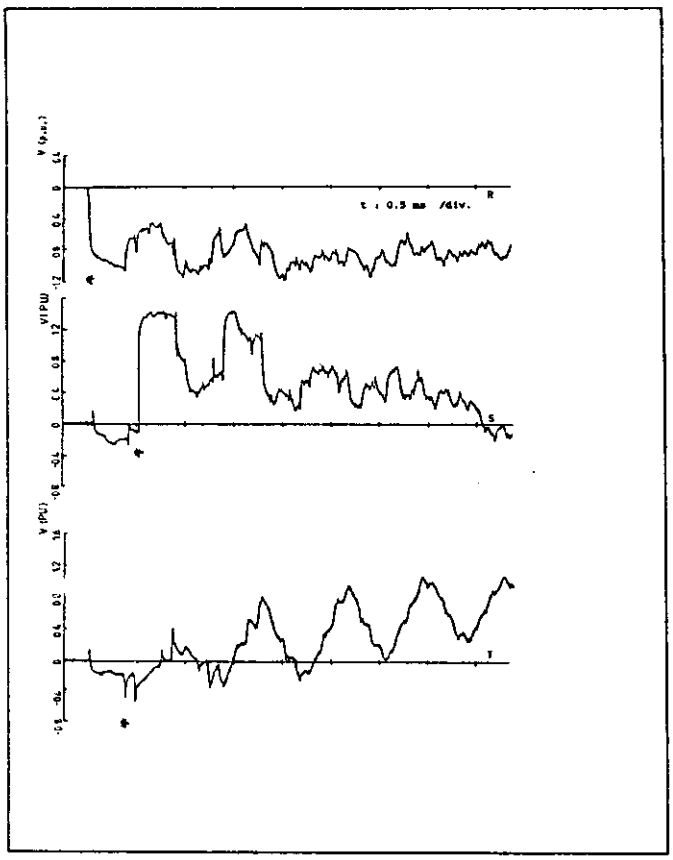

TNA Simulation

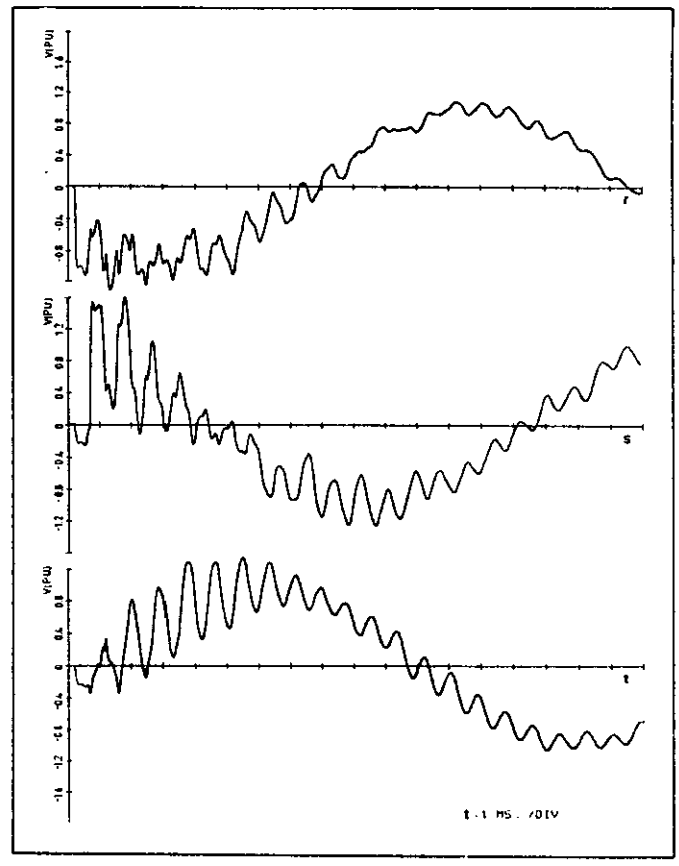

EMTP-I Calculations

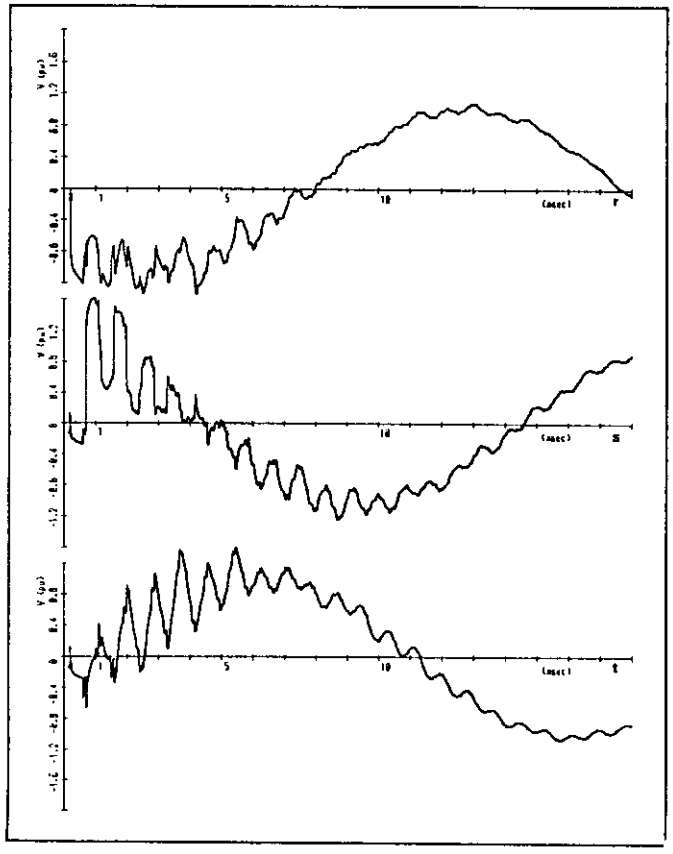

EMTP-II Calculations

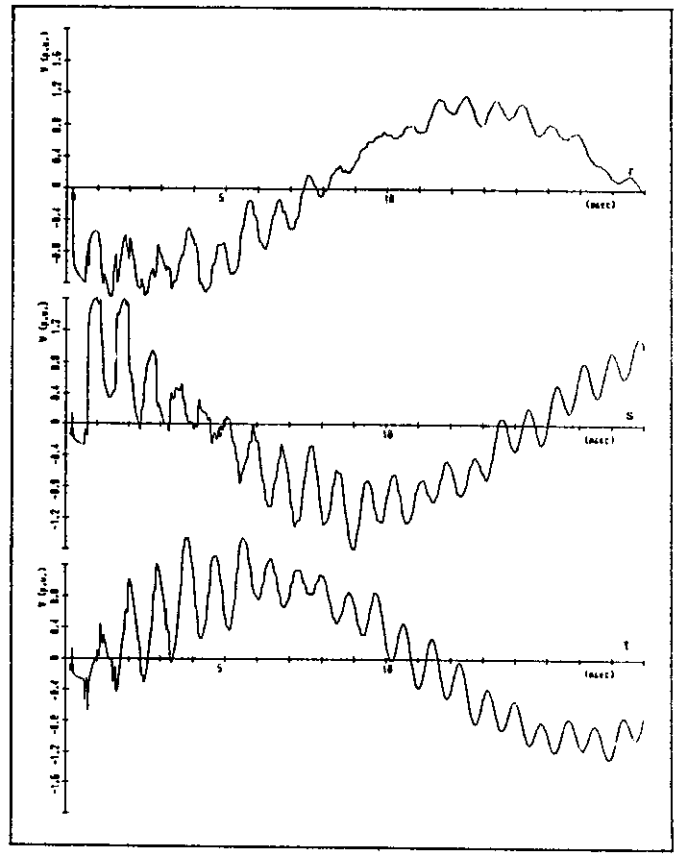

Figure 18 . Receiving-end overvoltages in Krimpen of test K 9

KEMA field test

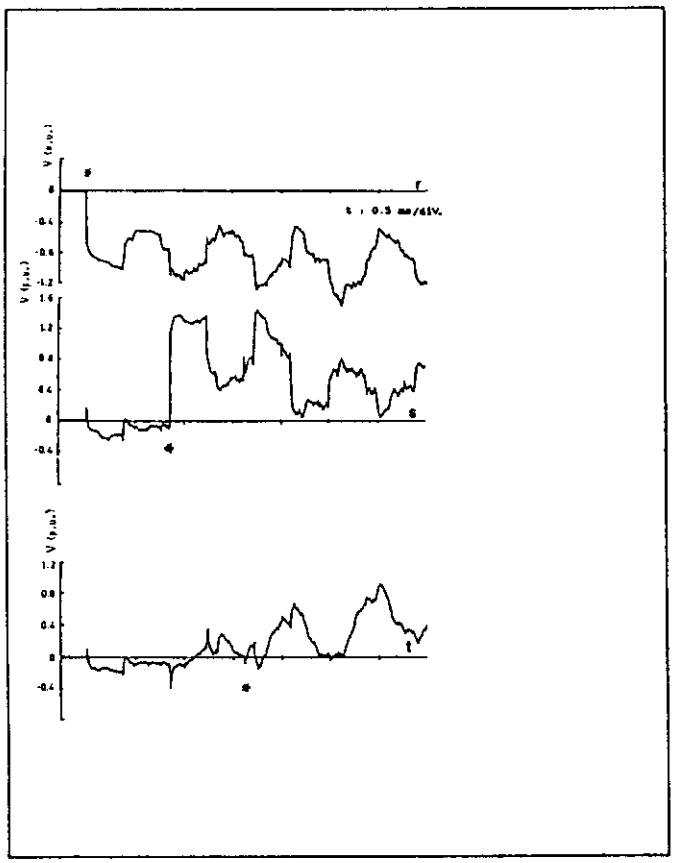

TNA Simulation

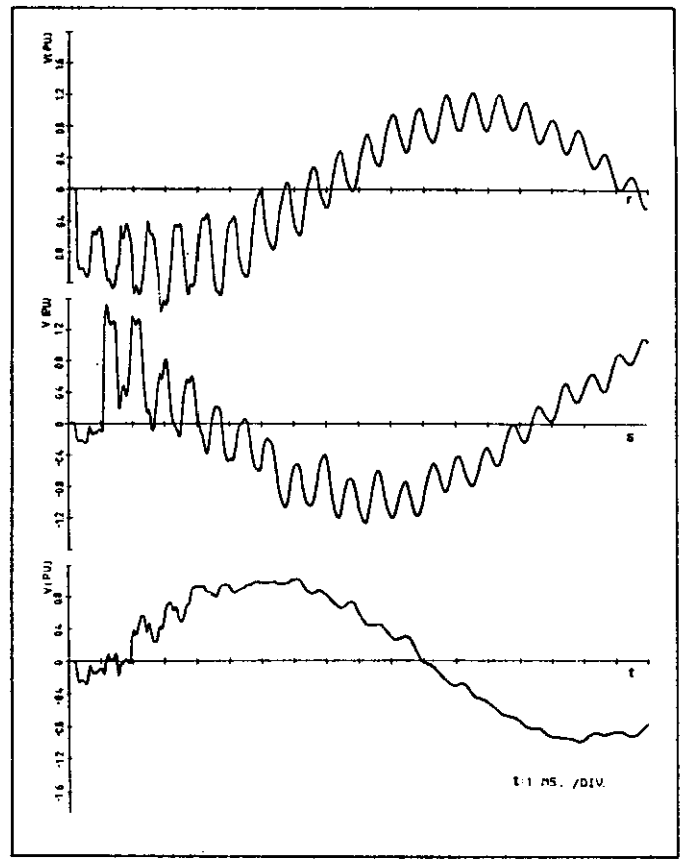

EMTP-I Calculations

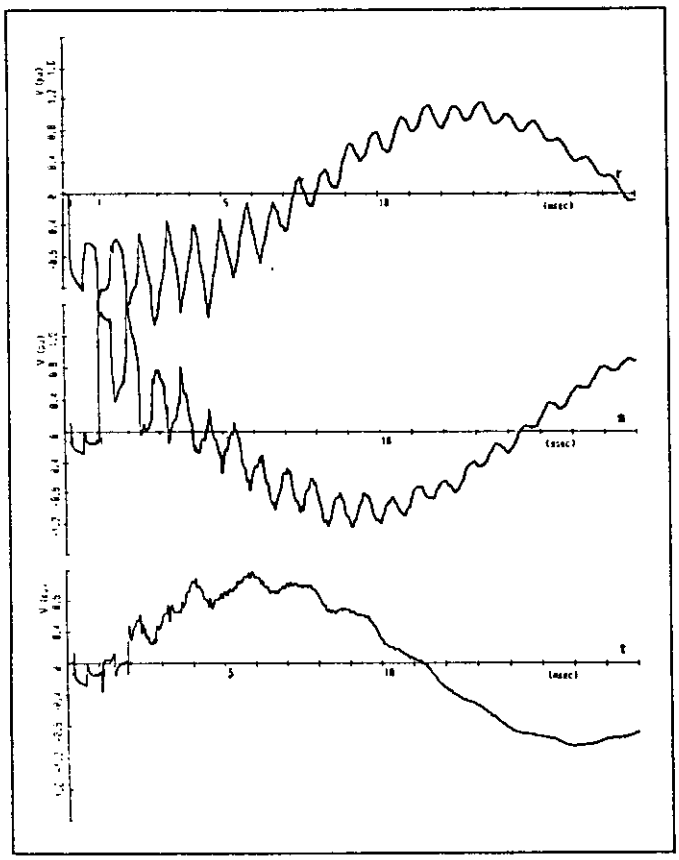

EMTP-II Calculations

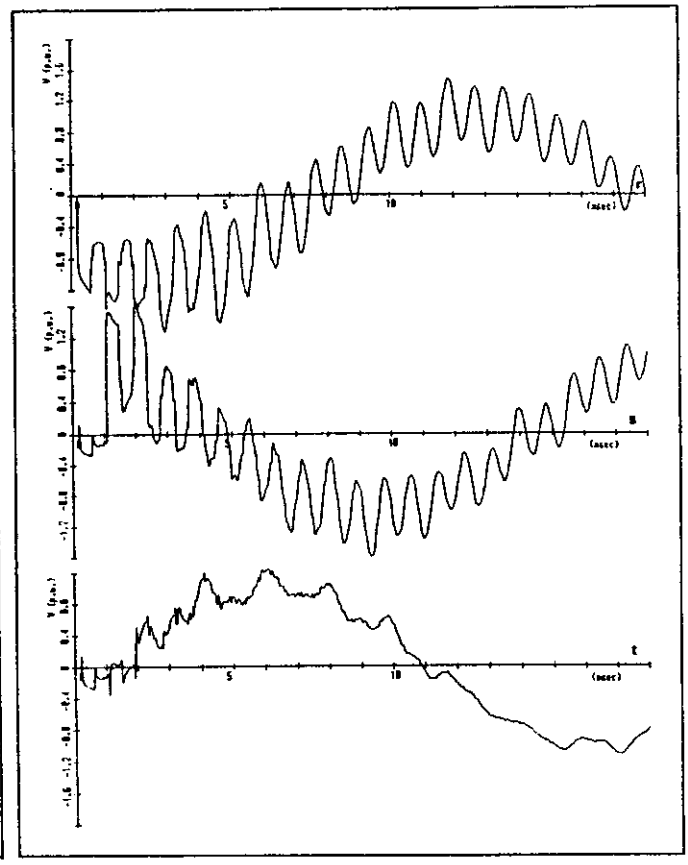

Figure 19 . Receiving-end overvoltages in Krimpen of test K 10

KEMA field test

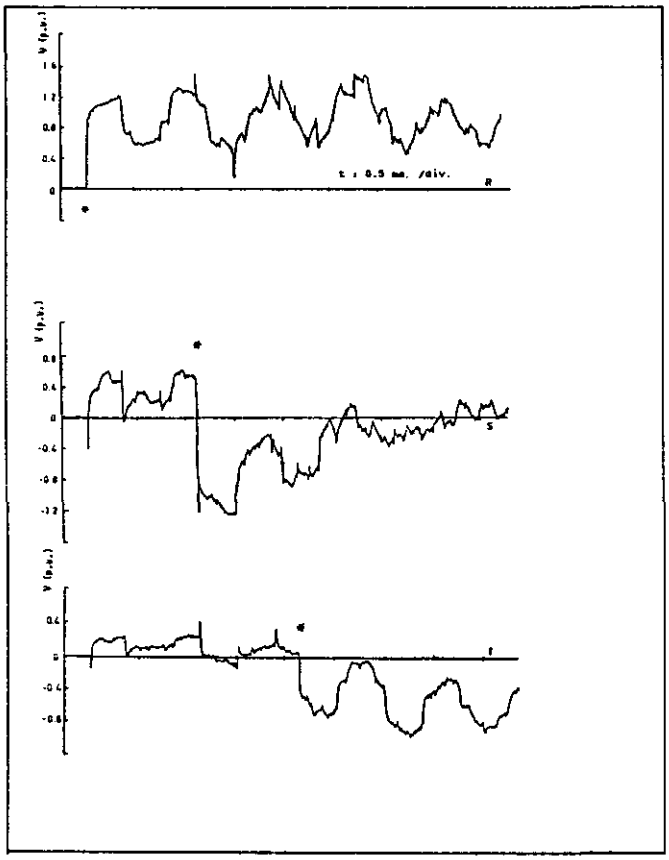

TNA Simulation

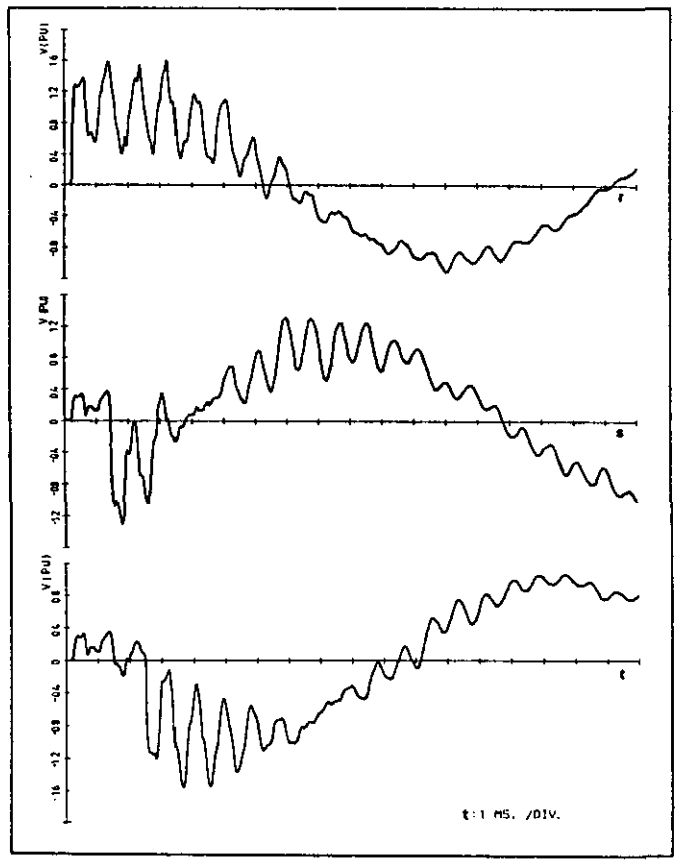

EMTP-I Calculations

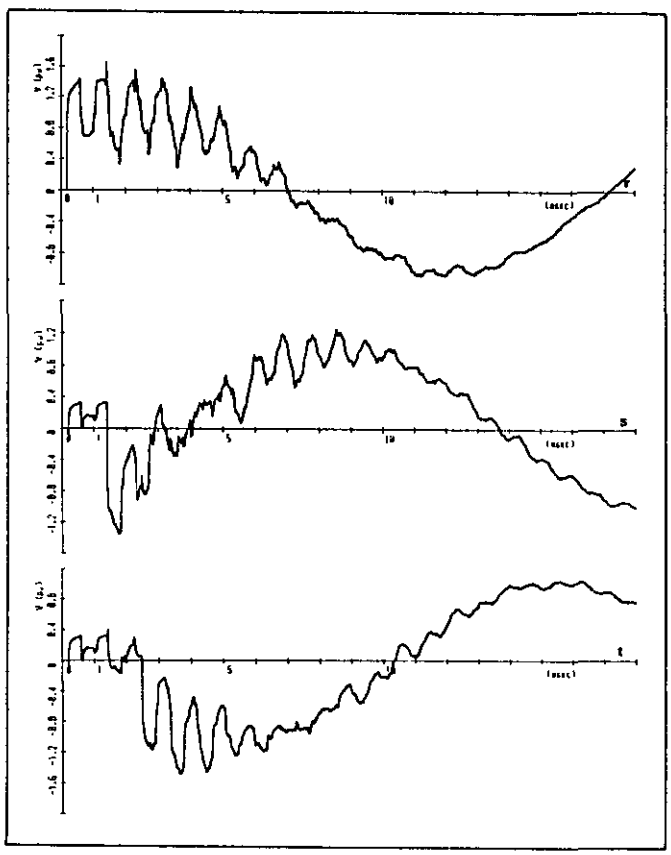

EMTP-II Calculations

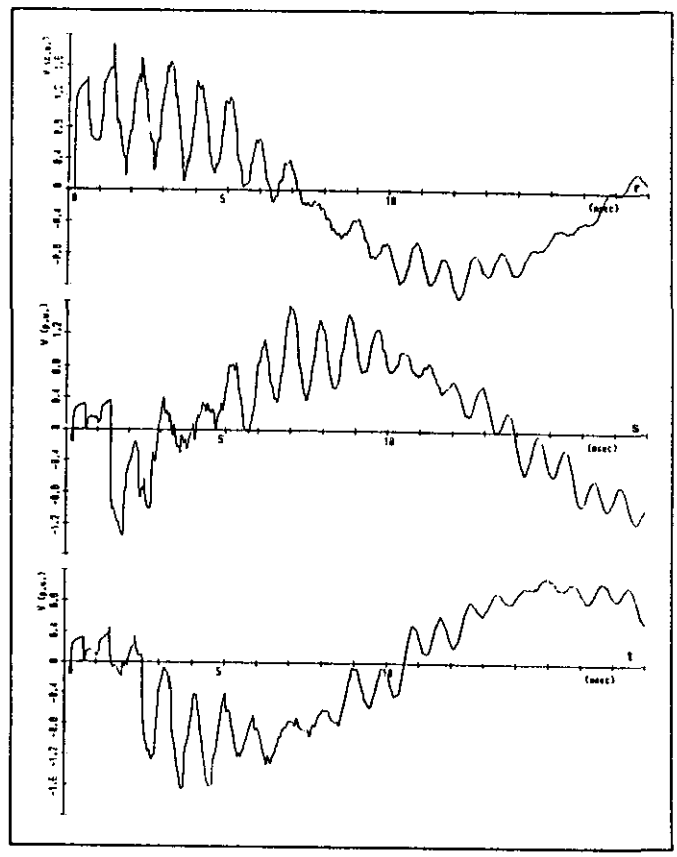

Figure 20 . Receiving-end overvoltages in Krimpen of test K 11

KEMA field test

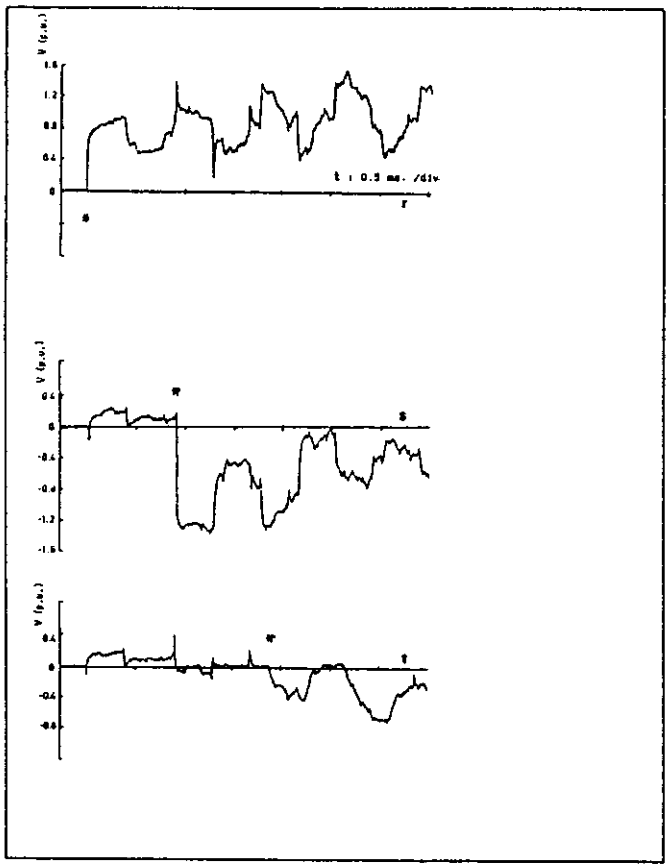

TNA Simulation

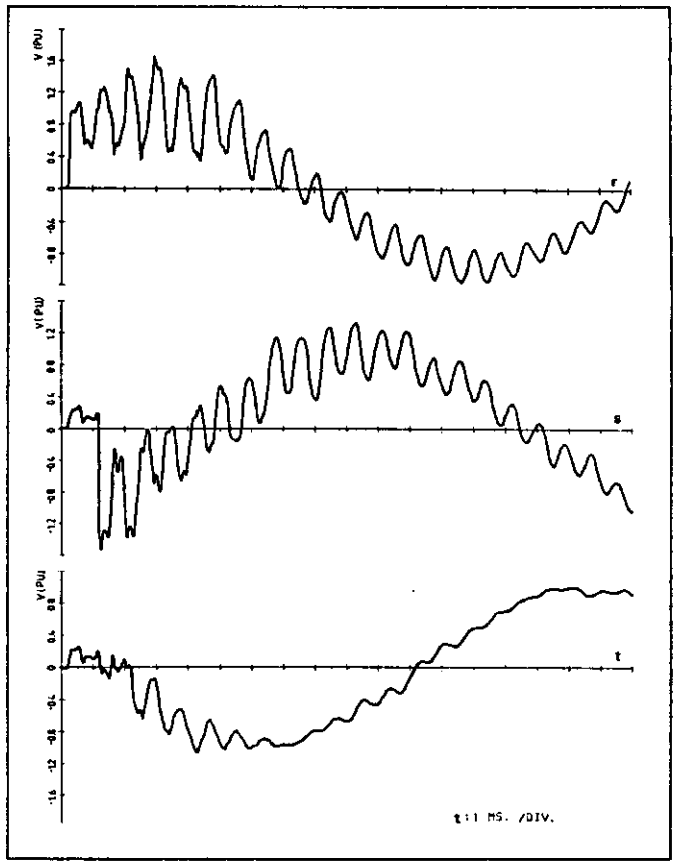

EMTP-I Calculations

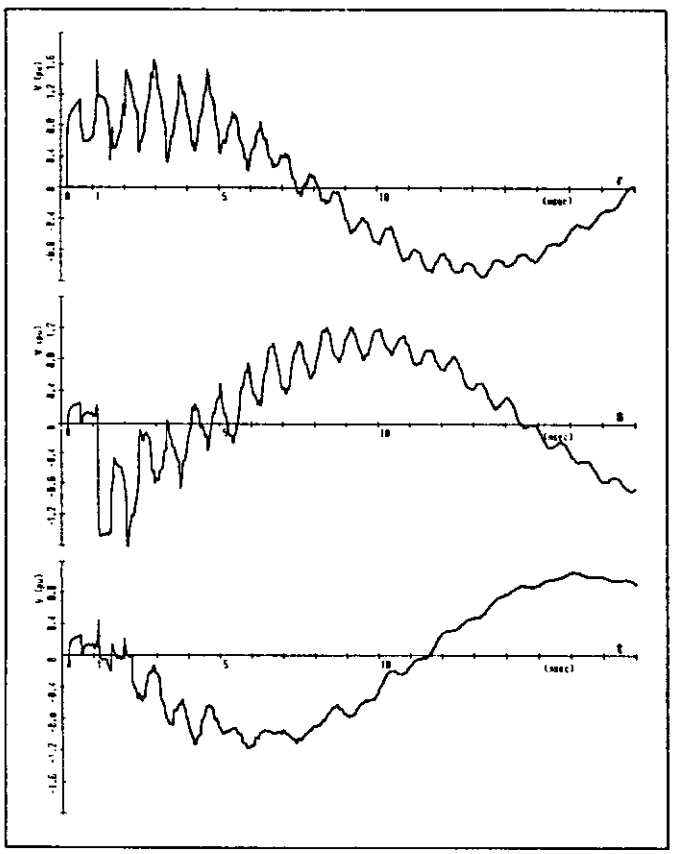

EMTP-II Calculations

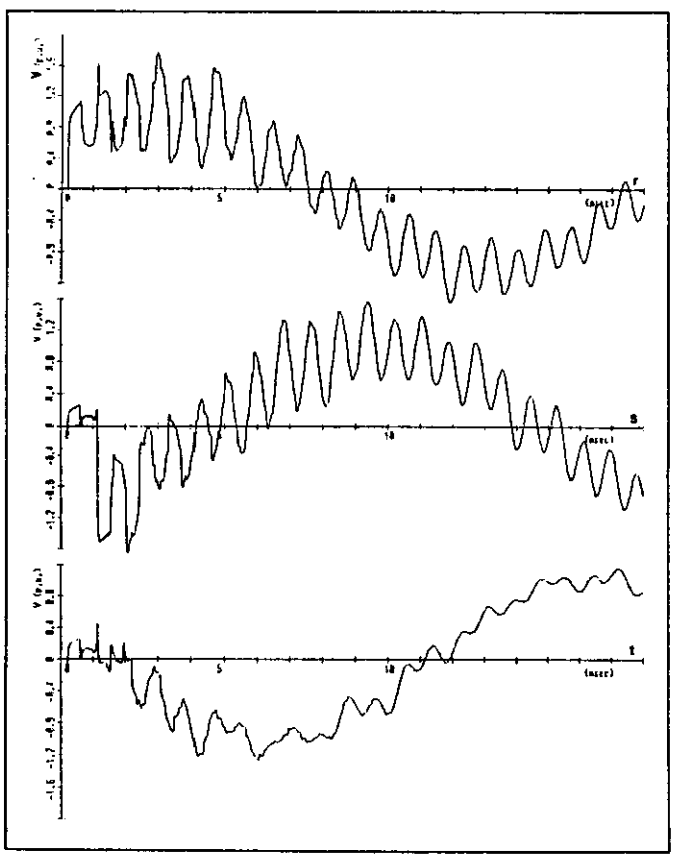

Figure 21 . Receiving-end overvoltages in Krimpen of test K 12

KEMA field test

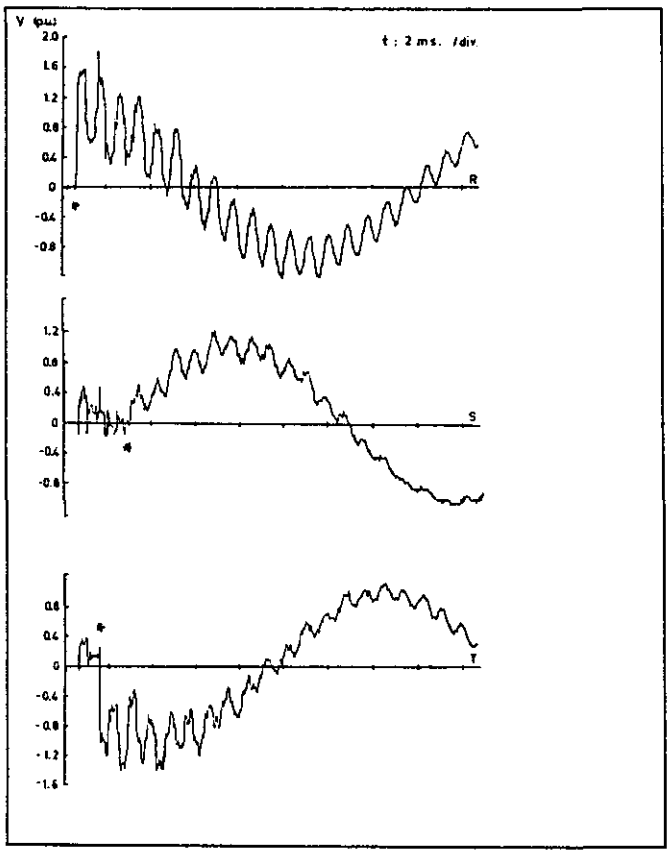

TNA Simulation

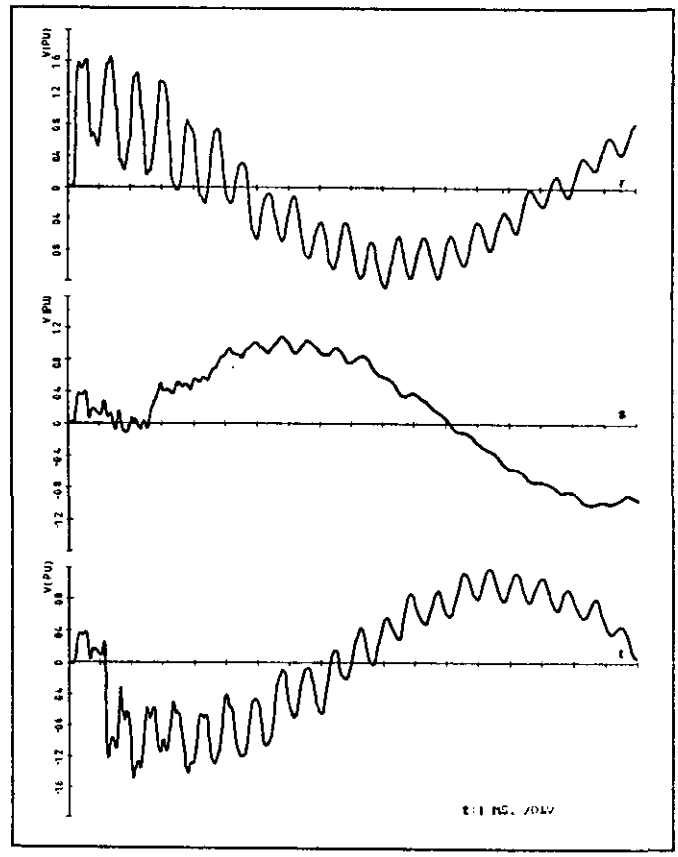

EMTP-I Calculations

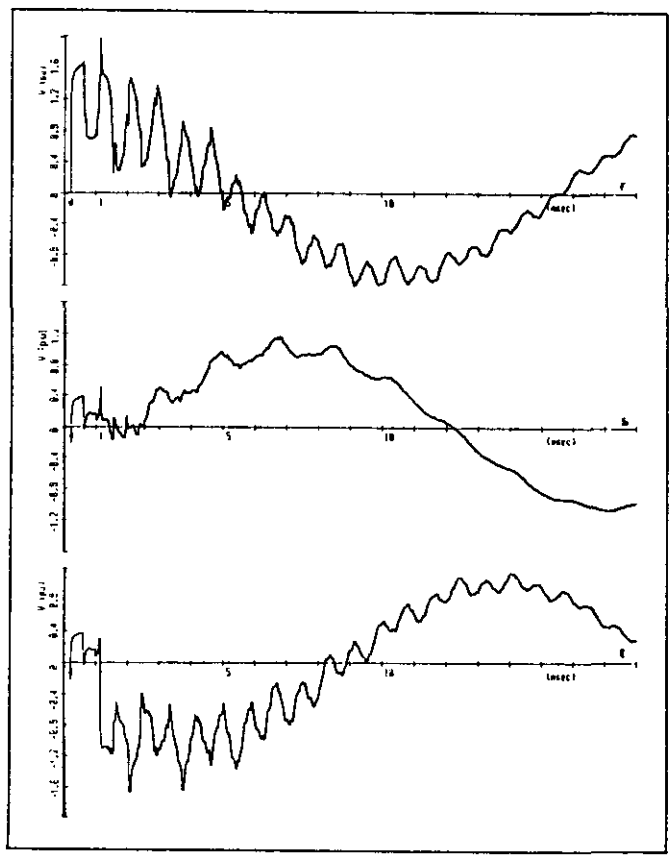

EMTP-II Calculations

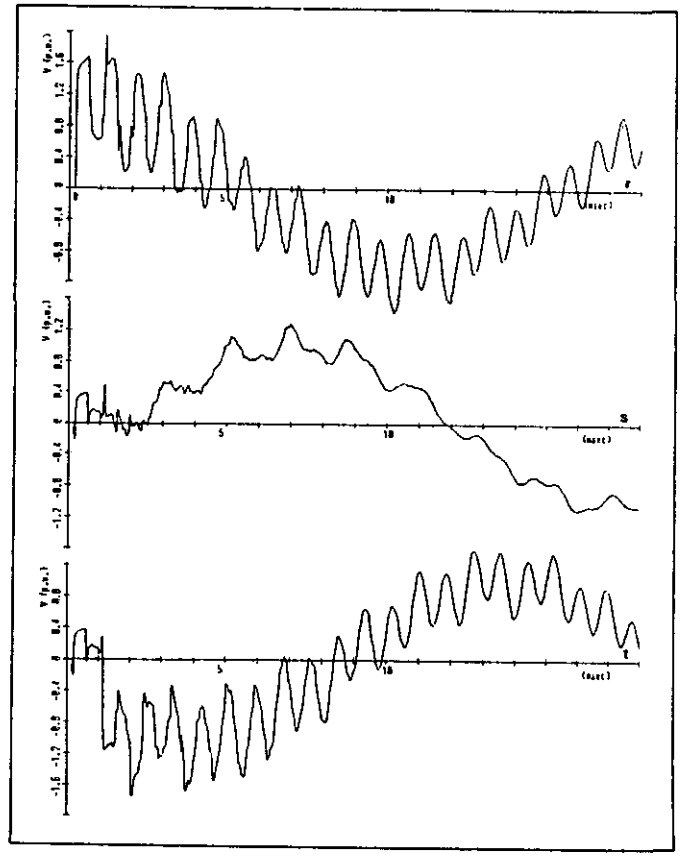

Figure 22 . Receiving-end overvoltages in Krimpen of test K 13

KEMA field test

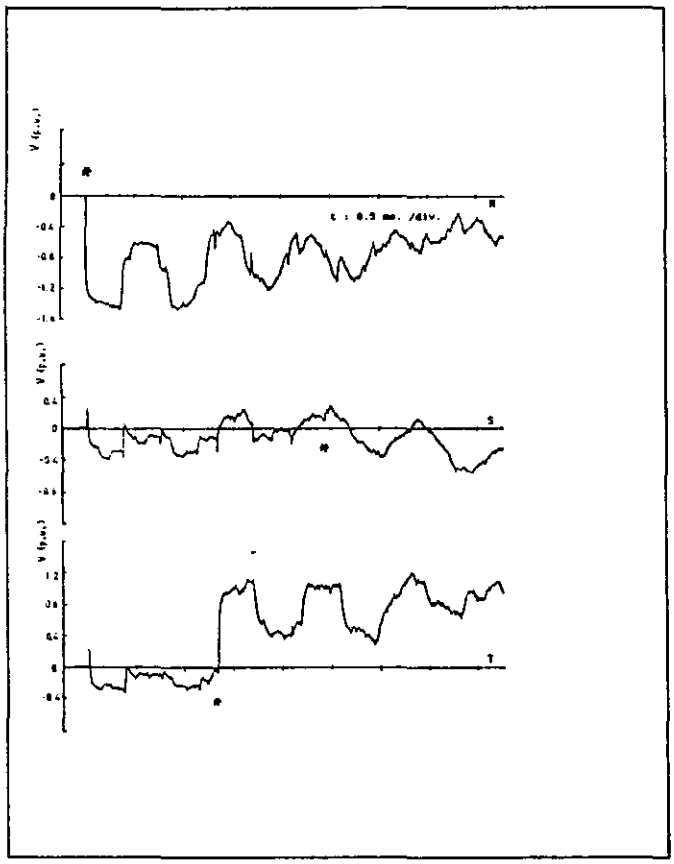

TNA Simulation

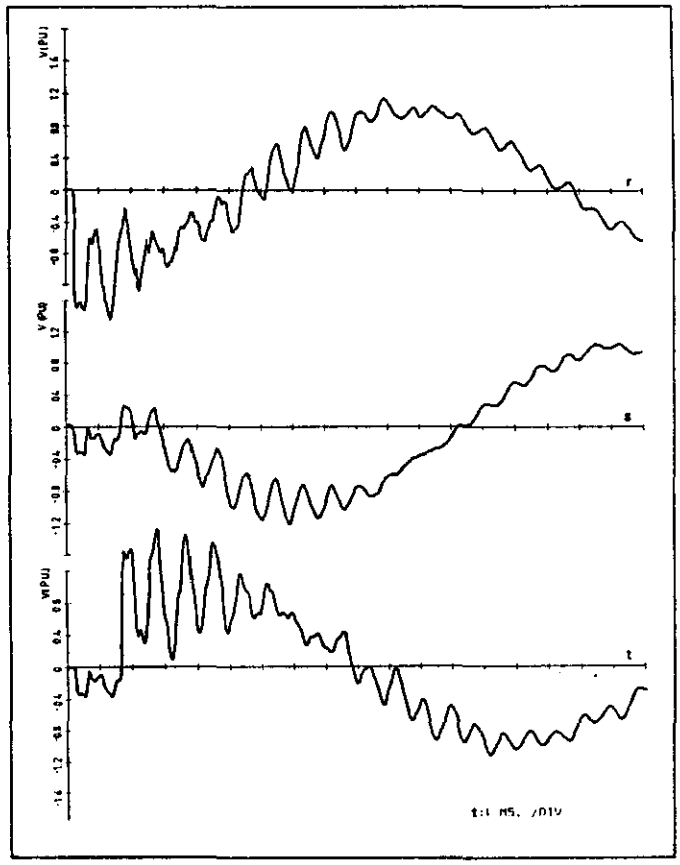

EMTP-I Calculations

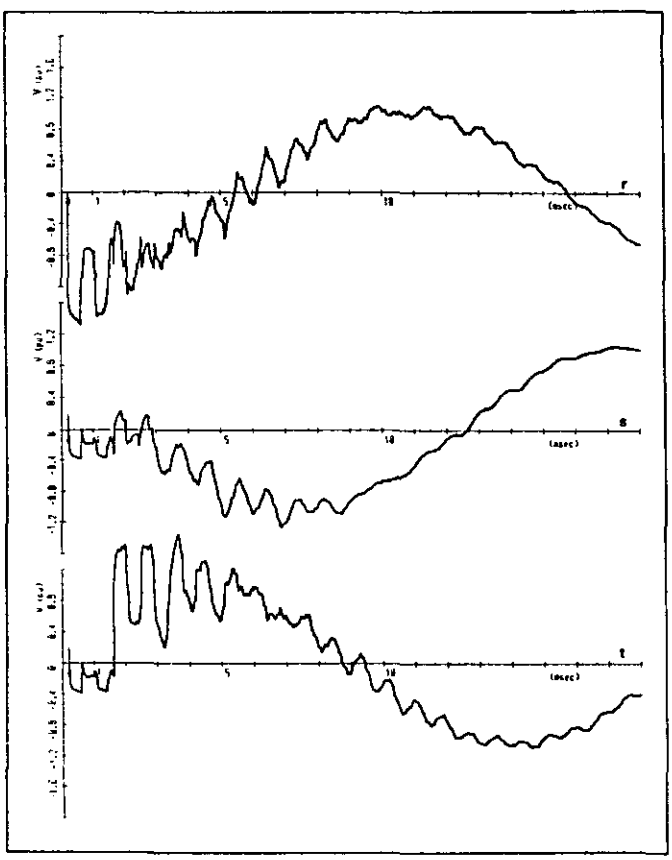

EMTP-II Calculations

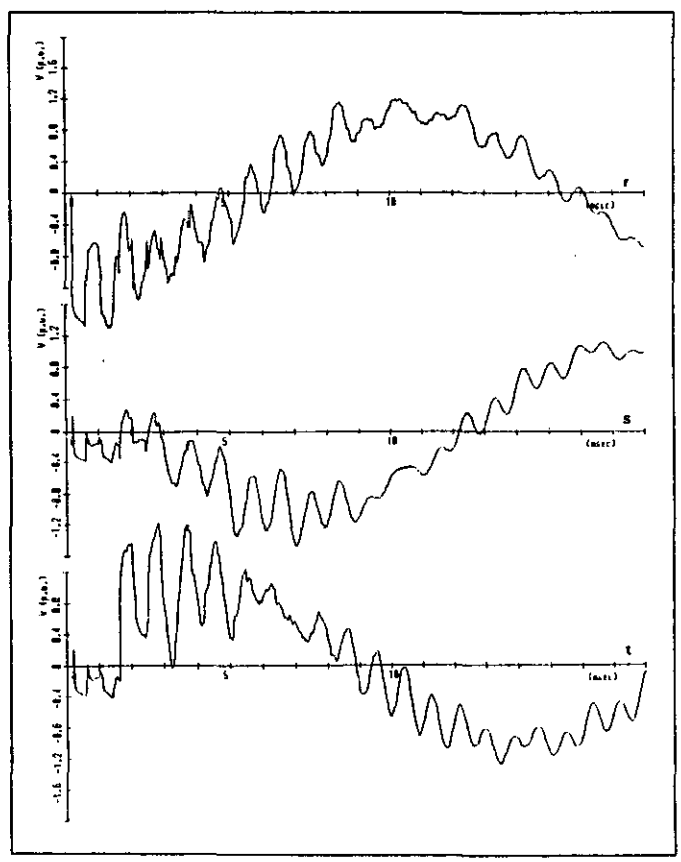

Figure 23 . Receiving-end overvoltages in Krimpen of test K 14

KEMA field test

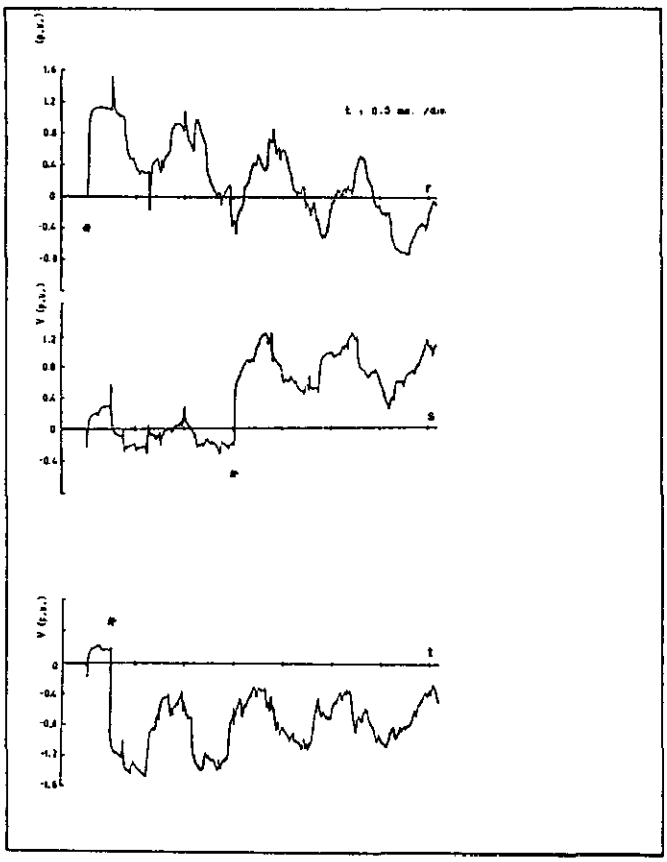

TNA Simulation

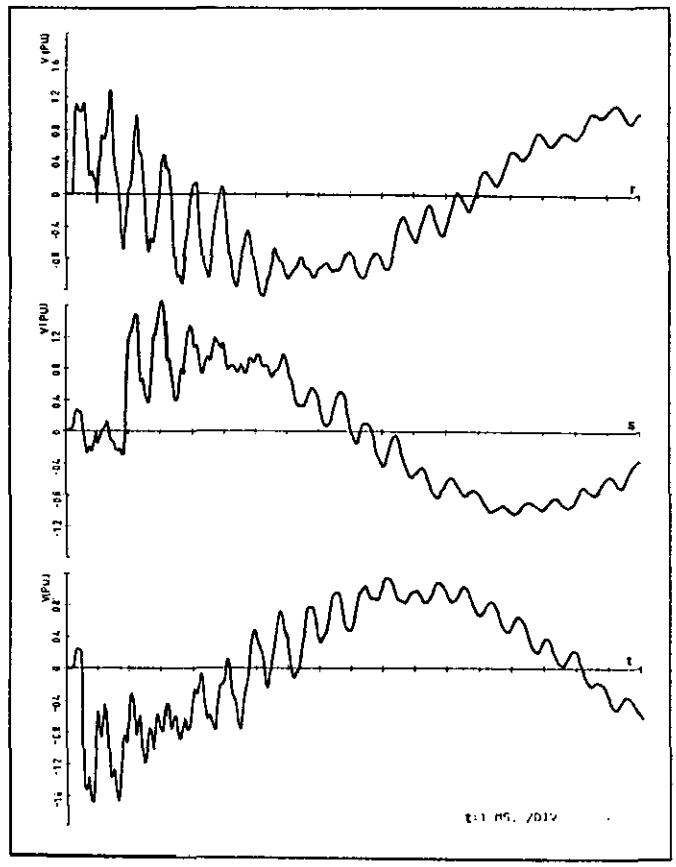

EMTP-I Calculations

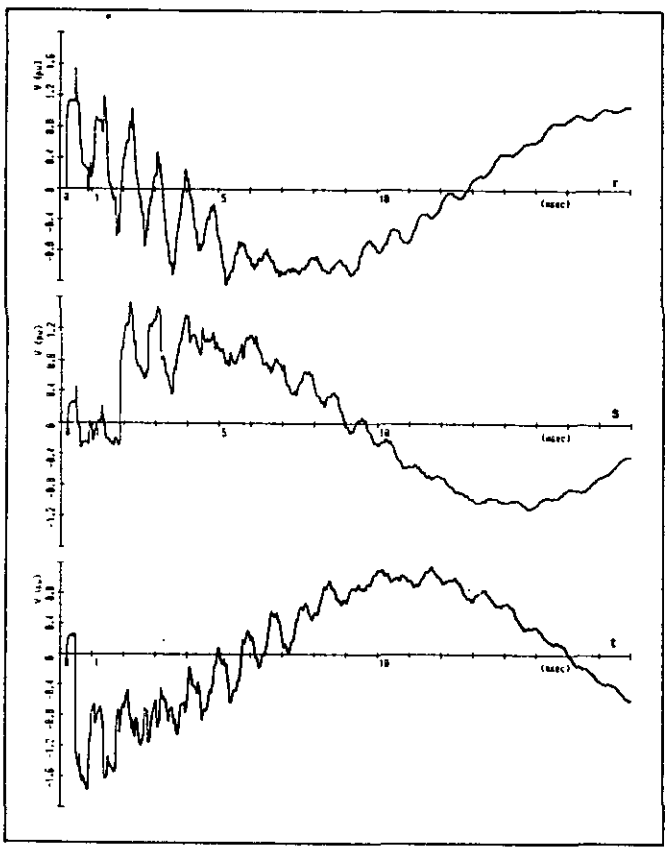

EMTP-II Calculations

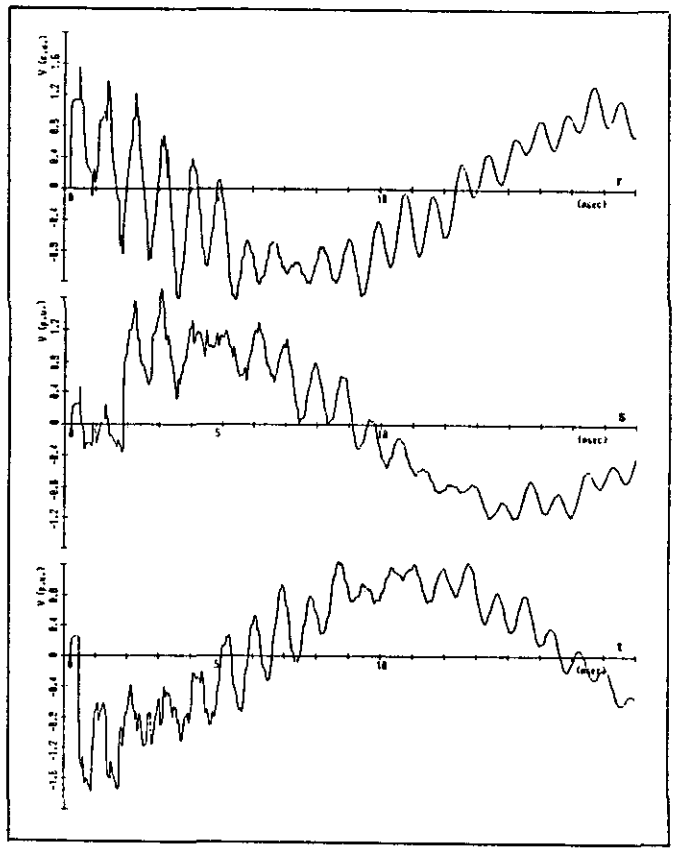

However the damping of the predominant oscillations is too low in the EMTP-II plots , see e.g. Figure 11 . The waveforms obtained by TNA simulation follow the pattern of the measured waveforms quite well , however , the high frequency components are rapidly damped . Also the voltage spikes at the moments of switching , clearly observable in the field records and in the EMTP plots , are not present . These spikes , caused by the slower propagation speed of the ground mode in comparison with the aerial modes , are beyond the frequency range of the TNA .

Looking in detail at the initial waveforms after first pole closing, it can be observed that irregularities present in the field records of both not yet closed phases are not present in the simulation results .

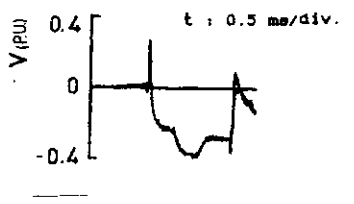

Figure 24 .

As an example Figure 24 shows the enlarged initial waveform of field test K13 ,phase S. The clearly observable voltage jumps are due to reflections at the two transposition points of the switched line . These transpositions were not modelled .

In some field tests the highest voltage appeared at the first voltage jump while in other tests more than ten milliseconds had been passed . So , when simulating line energizations , not only the initial transients but the waveforms during one cycle of power frequency are of interest in order to obtain the correct overvoltage peak values . From the field records it can be observed that the initial steep surges change into single frequency oscillations which are damped out . Incorrect damping of these oscillations in the simulations results in wrong overvoltage peak values . Comparing the waveforms of field tests K1 , K6 and K12 with the corresponding simulations it can be observed that the damping of the predominant oscillations in TNA and EMTP-I over -voltages is in agreement with the field tests quite well . As already discussed in chapter 4 the overvoltages calculated by EMTP-II show predominant oscillations with higher initial amplitudes and lesser damping .

The correspondance mentioned above should be confirmed by comparing the overvoltage peak values . The measured and calculated values have already been listed in Tables 1 ,3 , 4 and 5 together with their mean values and standard deviations . The latter are summarized in Table 6 .

test	mean value	standard deviation	2 % overvoltage
field	1.461 p.u.	0.197 p.u.	1.87 p.u.
EMTP-I	1.531 p.u.	0.224 p.u.	1.99 p.u.
EMTP-II	1.632 p.u.	0.194 p.u.	2.03 p.u.
TNA	1.487 p.u.	0.215 p.u.	1.93 p.u.

Table 6 . Statistical data of measured and simulated overvoltage peak values

In Figure 25 the overvoltage values are presented by means of cumulative frequency distribution curves . The best correspondance with the field test distribution curve has been achieved by TNA simulation , despite its limited frequency range . In the upper overvoltage range the distribution curves of both EMTP simulations approach each other . This is easy to explain as the highest overvoltages occured within 2 ms after first pole closing . The difference in damping of the predominant oscillations has affected the peak values of these overvoltages only to a small extent . In the lower overvoltage range the lower damping in the EMTP-II simulations is responsible for the increasing difference between both distribution curves .

Some caution is desired not to overestimate the conclusions derived from a comparison of the overvoltage distribution curves . Only 13 field tests were suitable for analysis and simulation so to each derived peak value a 3.3 % probability of occurance has been assigned . Measuring errors , less accurate network data and differences in switching moments certainly have introduced some inaccuracies . As an example , the highest peak value of all simulations has been generated in test K4 , phase T , at the moment the third pole closed causing an

additional increase of the already high momentary voltage . Such an increase cannot be observed in the field record (Figure 13) and therefore its overvoltage is quite moderate .

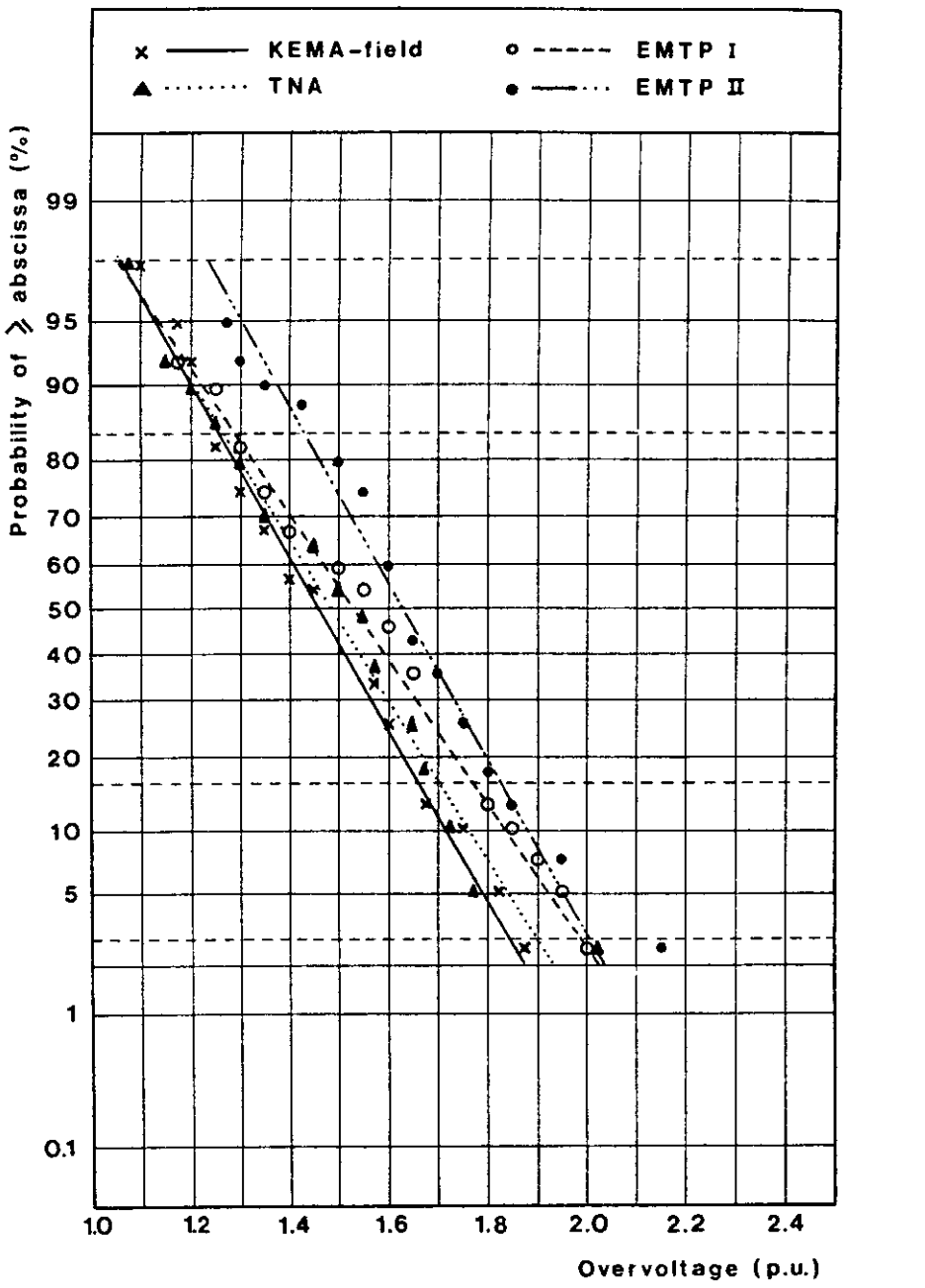

Figure 25 . Cumulative distribution of overvoltage peak values

A small shift in the closing moments applied in the simulations could easily have changed this view .

Another way to evaluate the simulation results is by individual comparison of the results . The difference between each overvoltage peak value obtained by simulation and its value in the field test have been determined . The statistical distribution of these differences are shown as histograms in Figure 26 , 27 and 28 for respectively EMTP-I , EMTP-II and TNA . The dispersion between the overvoltage peak values of the simulations and the field data is the smallest for EMTP-I . Nevertheless the mean difference of 0.07 p.u. is somewhat higher than that of the TNA results, 0.026 p.u. , but the standard deviation is smaller. Of all EMTP-I data 80 % have a difference against the corresponding field data within $\pm$ 0.15 p.u. being 10 % of the mean value of the overvoltages . The largest difference is 24 % and concerns the highest overvoltage in all simulations (test K4 , phase T) . It can be seen in Figure 28 that the differences between TNA and field test results are equally distributed over the positive and the negative region . This explains the good correspondance between both overvoltage distribution curves in Figure 25 .

Based on the statistical data as given in Table 6 the overvoltage peak value with 2 % probability of exceeding has been calculated and given in the same table . These so called " statistical overvoltages " are all in the range 1.95 $\pm$ 4 % p.u. .

In order to check whether the results of field tests and simulations are representative of line energizing overvoltages in the line of concern , a test of 100 closing operations was performed on the TNA . The closing instants applied were identical to those used in Cigré WG 13.05 for the comparison of different TNA 's [2]. The 300 overvoltage peak values had a mean value of 1.48 p.u. and a standard deviation of 0.243 p.u. . The statistical overvoltage was 1.98 p.u. . These data are well in accordance with the results of field tests and simulations presented in Table 6 .

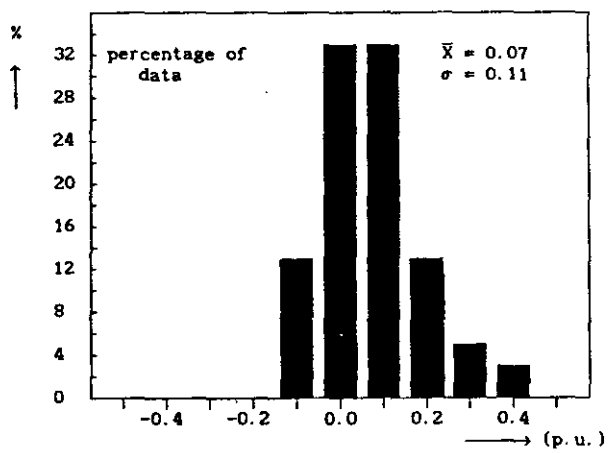

Figure 26 . Distribution of individual differences between EMTP-I and field tests

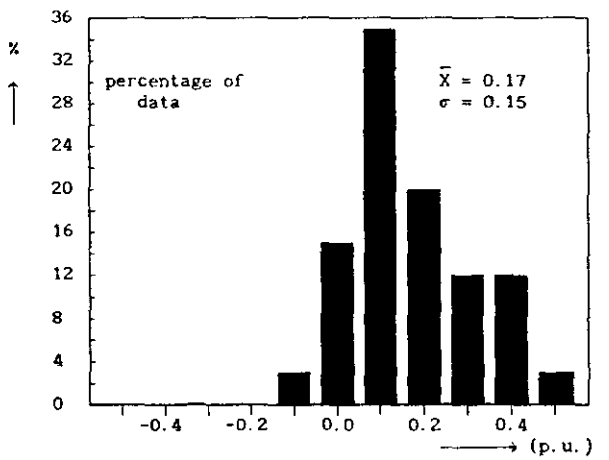

Figure 27 . Distribution of individual differences between EMTP-II and field tests

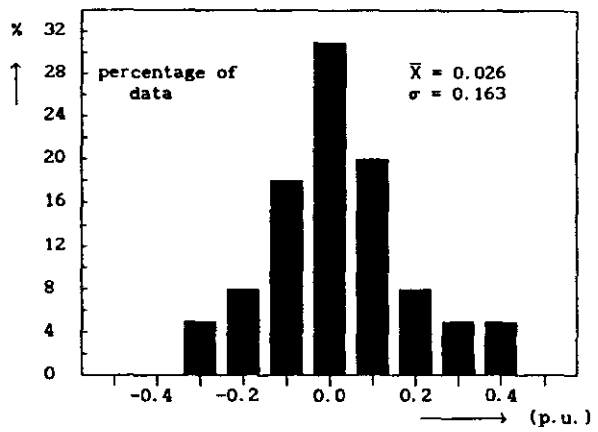

Figure 28 . Distribution of individual differences between TNA and field tests

7 Conclusions

The overvoltages due to the energization of unloaded overhead lines can be predicted rather accurately by simulation on a transient network analyzer and by calculation with EMTP . The duplication of thirteen field tests has yield waveforms and overvoltage peak values well in accordance with the field measurements .

The duplication of a particular field test requires an exact determination of the closing moments . Small deviations in closing moments can largely affect waveforms and voltage peaks .

Voltage waveforms with the best resemblance to the field test records have been obtained by EMTP calculations . This applies especially to the first milliseconds , where multiple reflections determine the waveform .

The initial steep voltage surges transit into a predominant oscillation superimposed on the 50 Hz waveform . The damping of the oscillations affects the overvoltage peaks arising after some milliseconds . The initial calculations by EMTP , called EMTP-II , produced voltage waveforms with less damping of these oscillations . After modification of the representation of the feeding network in substation Ens , the damping was quite well in accordance with the field test records . This finding supports the general experience that computer calculations can result in somewhat higher overvoltages .

Due to the inherent damping of the analog network models the waveforms produced by TNA show predominant oscillations well in acccordance with the field tests . However this inherent damping and the limited bandwidth of the models have limited the generation of spikes and h.f. components .

The cumulative distribution of overvoltage peak values obtained by TNA shows the best correspondance to that of the field tests . Both EMTP simulations have produced somewhat higher peak values in the upper overvoltage range .

The dispersion between the overvoltage peak values of the simulations and of the field tests is the smallest for EMTP-I simulations .

The results indicate that even differences in peak values up to 24 % can result in nearly equal cumulative distribution curves .

The overvoltage peak values with 2 % probability of exceeding of all distribution curves are within the range 1.95 $\pm$ 4 % p.u. .

---

8 References

[1] Clerici , A .
ANALOG AND DIGITAL SIMULATION FOR TRANSIENT OVERVOLTAGE DETERMINATIONS .
Electra (Paris) , No. 22 (1972) , p. 111 - 138 .

[2] THE CALCULATION OF SWITCHING SURGES . I : A comparison of transient network analyser results . CIGRÊ Working Group 13.05.
Chairman of the Committee 13 : H. Meyer .
Electra (Paris) , No. 19 (1971) , p. 67 - 78 .

[3] THE CALCULATION OF SWITCHING SURGES . II : Network representation for energization and re-energization studies on lines fed by an inductive source . CIGRÉ Working Group 13.05 .
Chairman of the Committee 13 : G. Catenacci .
Electra (Paris) , No. 32 (1974) , p. 17 - 42 .

[4] THE CALCULATION OF SWITCHING SURGES . III : Transmission line representation for energization and re-energization studies with complex feeding networks . CIGRÉ Working Group 13.05 .
Chairman of the Committee 13 : G. Catenacci .
Electra (Paris) , No. 62 (1979) , p. 45 - 78 .

[5] GUIDE FOR REPRESENTATION OF NETWORK ELEMENTS WHEN CALCULATING TRANSIENTS . CIGRÉ Working Group 33.02 .
CIGRÉ Internal Working Document , draft Jan. 1987 . To be published as a CIGRÉ Report .

[6] Foreman , K. et al.
ACCURACY OF RISK-OF-FAILURE CALCULATION AND SENSITIVITY TO VARIOUS INFLUENCING PARAMETERS .
In : Proc. Colloquium CIGRÉ Study Committee 33 (Overvoltages and Insulation Co-ordination) , Rio de Janeiro, 27-28 May 1981.

[7] Adami , H .
UITGEWERKTE RESULTATEN VAN DE OVERSPANNINGSMETING VAN 380 KV LIJN KRIMPEN-DIEMEN .
Arnhem : KEMA , 24 Oct . 1983 .
KEMA Report 13338 EO 8709-83 .

[8] Damstra , G.C.
OVERSPANNINGSMETINGEN 380 KV-STATIONS KRIMPEN A/D IJSSEL EN BORSSELE .
Arnhem : KEMA , 15 Dec . 1980 .
KEMA Report 94617 DZO-80-30 .

[9] Riet , M.J.M. van
HET SIMULEREN VAN HOOGSPANNINGSLIJNEN IN EEN TRANSIËNT NETMODEL
M.Sc. thesis .Electrical Energy Systems Division , Faculty of Electrical Engineering , Eindhoven University of Technology , 1979 .
EO.79.A.30

[10] Achten , W.G.J.
HET ONTWERPEN VAN EEN ANALOOG MODEL VAN EEN DUBBELCIRCUIT 380 KV LIJN T.B.V. TRANSIËNTE STUDIES .
Graduate Report Hogere Technische School Venlo , 1979 .
E79-16

[11] Geelen , W.H.
DE REPRESENTATIE VAN MEERVOUDIGE INVOEDINGEN IN EEN TRANSIËNT NETMODEL .
M.Sc. thesis . Electrical Energy Systems Division , Faculty of Electrical Engineering,Eindhoven University of Technology,1980.
EO.80.A.32

[12] Vernooy , M.G.
METHODE TER BEHANDELING VAN UITGESTREKTE NETTEN BIJ DE BEREKENING VAN OVERGANGSVERSCHIJNSELEN .
M.Sc.thesis . Electrical Energy Systems Division , Faculty of Electrical Engineering,Eindhoven University of Technology,1982.
EO.82.A.36

[13] Bun , R.M.P.
HET DIGITAAL BEREKENEN VAN OVERSPANNINGEN T.G.V. INSCHAKEL-HANDELINGEN MIDDELS RECURSIEVE CONVOLUTIE .
M.Sc. thesis . Electrical Energy Systems Division , Faculty of Electrical Engineering,Eindhoven University of Technology,1983.
EO.83.A.39

[14] ELECTROMAGNETIC TRANSIENTS PROGRAM [EMTP] . Rule Book .
Rev. version June 1984 .
Methods Development Branch , Route EOGB , Division of System Engineering , Bonneville Power Administration , P.O. Box 3621 , Portland , Oregon 97208 , USA .

[15] Birkhölzer , W.A.
IMPEDANTIE-EN CAPACITEITEN-MATRICES VAN HOOGSPANNINGS-VERBINDINGEN VOOR EEN UITGEBREID FREQUENTIEGEBIED .
M.Sc. thesis . Electrical Energy Systems Division , Faculty of Electrical Engineering,Eindhoven University of Technology,1977.
EO.77.A.26

[16] Michelis , E.J.
VERGELIJKING TUSSEN METING EN BEREKENING BIJ HET INSCHAKELEN VAN DE LIJN DIEMEN-KRIMPEN MET EEN COMPLEXE BRON EN DE INVLOED VAN DE MODELLERING VAN DE NETELEMENTEN OP DE VORM EN DE AMPLITUDE VAN DE OVERSPANNINGEN .
Arnhem : KEMA , 2 Sept. 1987 .
KEMA Report 20496 EO 87-3037

[17] Michelis , E.J.
COMPARISON BETWEEN MEASUREMENT AND CALCULATION OF LINE SWITCHING WITH INDUCTIVE AND COMPLEX SOURCE .
Paper 88 SM 588-6 presented at the IEEE/PES 1988 Summer Meeting , Portland , Oregon , 24-29 July 1988.

[18] Dommel , H.W.and W.S. Meyer
COMPUTATION OF ELECTROMAGNETIC TRANSIENTS .
Proc. IEEE , Vol. 62 (1974) , p. 983 - 993 .

[19] Marti , J.R.
ACCURATE MODELLING OF FREQUENCY-DEPENDENT TRANSMISSION LINES IN ELECTROMAGNETIC TRANSIENT SIMULATIONS .
IEEE Tran.Power Appar. & Syst., Vol. PAS-101 (1982) ,p 147-157 .

[20] Marti ,J.R. , H.W. Dommel , L. Marti , and V. Brandwajn.
APPROXIMATE TRANSFORMATION MATRICES FOR UNBALANCED TRANSMISSION LINES .
In : Proc. 9th Power Systems Computation Conf. (PSCC) , Cascais , Portugal , 30 Aug. - 4 Sept. 1987 .
London : Butterworth , 1987 . P. 416 - 422 .

[21] Ritchie , W.M. and J.T. Pender
THE MODERN TRANSIENT NETWORK ANALYSER AND ITS ROLE IN ANALYSIS AND DESIGN OF ELECTRICAL SYSTEMS .
Proc. Inst. Electr.Eng. (London) , Vol. 125 (1978), p. 129-134 .

[22] Clerici , A. and L. Marzio
COORDINATED USE OF TNA AND DIGITAL COMPUTER FOR SWITCHING-SURGE STUDIES : transient equivalent of a complex network .
IEEE Trans. Power Appar. & Syst. , Vol. PAS-89 (1970) , p. 1717-1726 .

type 3

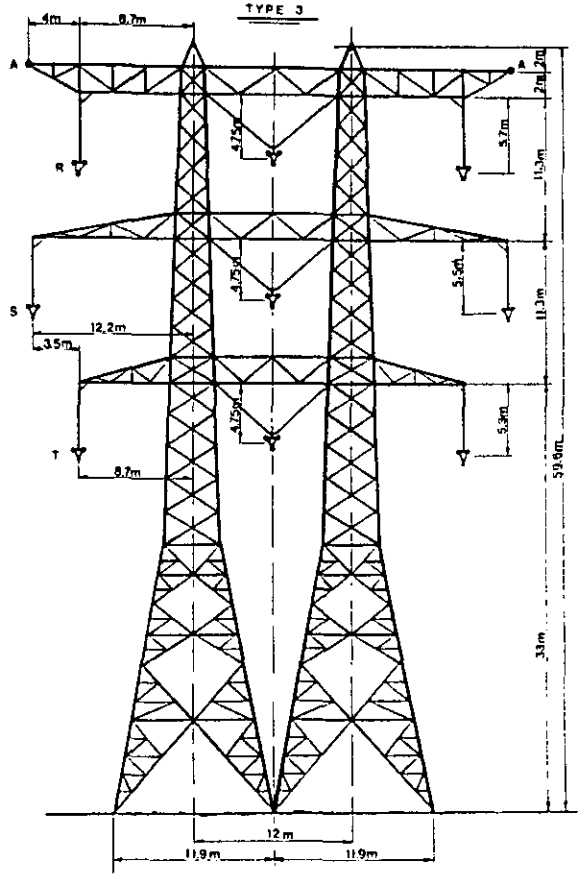

conductor bundle 3*424/39 mm^2 Al/St
A : ground wire 1*242/39 mm^2 Al/St

type 1 , 4

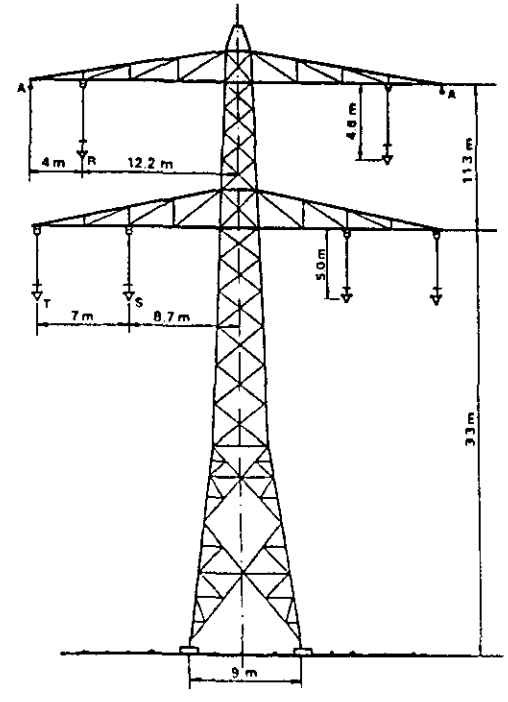

type 1

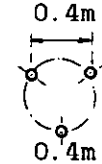

conductor bundle 3*423/37 mm^2 Al/St
A : ground wire 1*242/39 mm^2 Al/St

type 4

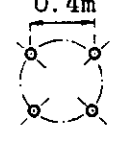

conductor bundle 4*591/52 mm^2 Al/St
A : ground wire 1*242/39 mm^2 Al/St

Configuration tower type 1

Tower type 1 is a standard two circuit system with two ground wires and six bundle conductors of three wires . The rotation angle is -90 degrees . The reference point for the horizontal distance is the middle of the tower . (the distances are measured from the reference point to the center of the bundle conductor) .

bundle/wire	horizontal distance [m]	center height at tower [m]	center height midspan [m]
left outside	-15.7	28.0	12.0
left up	-12.2	39.7	23.7
left inside	- 8.7	28.0	12.0
right inside	8.7	28.0	12.0
right up	12.2	39.7	23.7
right outside	15.7	28.0	12.0
left ground	-16.2	44.3	31.3
right ground	16.2	44.3	31.3

Configuration tower type 3

Tower type 3 is a three circuit system with two ground wires and nine bundle conductors of three wires . The rotation angle is - 90 degrees . The reference point for the horizontal distance is the left ground wire.

bundle/wire	horizontal distance [m]	center height at tower [m]	center height midspan [m]
left up	4.0	49.9	33.9
left middle	0.5	38.8	22.8
left down	4.0	27.7	11.7
middle up	18.7	50.85	34.85
middle middle	18.7	39.55	23.55
middle down	18.7	28.25	12.25
right up	33.4	49.9	33.9
right middle	36.9	38.8	22.8
right down	33.4	27.7	11.7
left ground	0.0	57.6	44.6
right ground	37.4	57.6	44.6

Configuration tower type 4

Tower type 4 is a heavy version of type 1 : 4 wire bundle conductors . The rotation angle is 45 degrees . The reference point for the horizontal distance is the left ground wire .

bundle/wire	horizontal distance [m]	center height at tower [m]	center height midspan [m]
left outside	0.75	29.0	13.0
left up	4.0	40.5	24.5
left inside	7.25	29.0	13.0
right inside	25.75	29.0	13.0
right up	29.0	40.5	24.5
right outside	32.25	29.0	13.0
left ground	0.0	46.5	33.5
right ground	33.0	46.5	33.5

Data of the conductors

d/D : is the ratio of the thickness of the tubular conductor and the outside diameter of the tubular conductor (aluminum) .
R : the resistance of the conductor in ohm/km .
D : the outside diameter of the tubular conductor in cm .
S : the distance between the conductor in the bundle in cm .
A : the angle between the horizontal axis and the first conductor of the bundle in degrees .
N : the number of conductors in the bundle .

Transmission line type 1

transmission line Diemen-Krimpen (distance 57.7 km.)
transmission line Diemen-Ens (distance 71.4 km)
transmission line Krimpen-Geertruidenberg (distance 32.7 km)
transmission line Eindhoven-Maasbracht (distance 48.2 km)

phase no.	d/D	R [ohm/km]	D [cm]	S [cm]	A [deg]	N
3	0.3575	0.06550	2.7850	40.0	-90	3
2	0.3575	0.06550	2.7850	40.0	-90	3
1	0.3575	0.06550	2.7850	40.0	-90	3
1	0.3575	0.06550	2.7850	40.0	-90	3
2	0.3575	0.06550	2.7850	40.0	-90	3
3	0.3575	0.06550	2.7850	40.0	-90	3
0(gnd)	0.3128	0.11334	2.1750			
0(gnd)	0.3128	0.11334	2.1750			

Transmission line type 3

Transmission line Geertruidenberg-Eindhoven(distance 64.24km)

phase no.	d/D	R [ohm/km]	D [cm]	S [cm]	A [deg]	N
1	0.3575	0.06550	2.7850	40.0	-90	3
2	0.3575	0.06550	2.7850	40.0	-90	3
3	0.3575	0.06550	2.7850	40.0	-90	3
1	0.3575	0.06550	2.7850	40.0	-90	3
2	0.3575	0.06550	2.7850	40.0	-90	3
3	0.3575	0.06550	2.7850	40.0	-90	3
1	0.3575	0.06550	2.7850	40.0	-90	3
2	0.3575	0.06550	2.7850	40.0	-90	3
3	0.3575	0.06550	2.7850	40.0	-90	3
0(gnd)	0.3128	0.11334	2.1750			
0(gnd)	0.3128	0.11334	2.1750			

Transmission line type 4

Transmission line Krimpen-Crayestein (distance 14.84 km)
Transmission line Crayestein-Maasvlakte (distance 66.4 km)

phase no.	d/D	R [ohm/km]	D [cm]	S [cm]	A [deg]	N
3	0.3578	0.04693	3.2900	40.0	45	4
2	0.3578	0.04693	3.2900	40.0	45	4
1	0.3578	0.04693	3.2900	40.0	45	4
1	0.3578	0.04693	3.2900	40.0	45	4
2	0.3578	0.04693	3.2900	40.0	45	4
3	0.3578	0.04693	3.2900	40.0	45	4
0(gnd)	0.3328	0.11334	2.1750			
0(gnd)	0.3328	0.11334	2.1750			

Data " LINE CONSTANTS "

Earth resistivity : 100 Ωm
Frequency range : 10^{1} - 10^{8} Hz

Data " JMARTI - SETUP "

Transformation matrix calculated at : 5 kHz
Characteristic impedance fitting ;

- error tolerance : 5 %
- allowed number of poles : 30

Weighting function fitting ;

- error tolerance : 8 %
- allowed number of poles : 25

Appendix 2 **Network data**

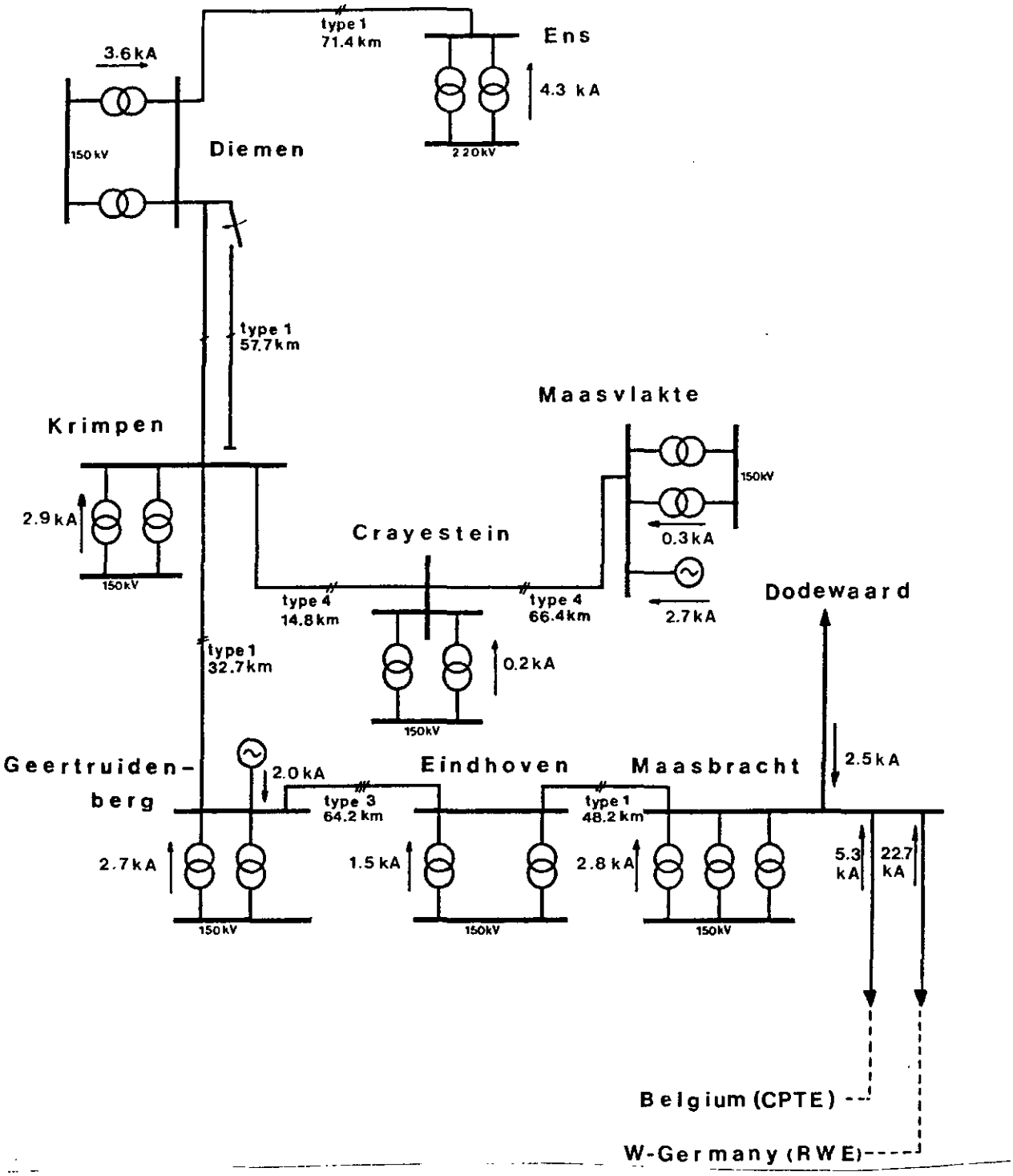

Figure 2-1 . Infeeding short-circuit currents (3 ph-fault)

Data of 400/150/50 kV transformers

Rated power (3 ph):	3 * 150 MVA	Vector group	: Y 0 y d 5
Rated voltages :	380 kV (UH)	Percentage imp.voltage ε_k:	UH-H, 18 %
	150 kV (H)		UH-L, 38 %
	50 kV (L)		H-L, 16.5%

Impedance diagram

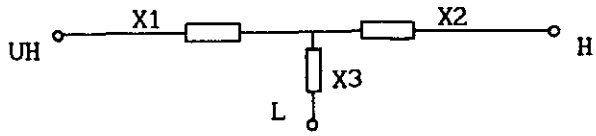

X1 = 63.4 Ω
X2 = -5.6 Ω
X3 = 58.6 Ω
on 380 kV basis

Data of substation Ens

Auto - transformers .		Vector group	: Y 0 d 5
Rated power :	500 MVA	Percentage imp.voltage ε_k:	UH-H, 14.3%
Rated voltages :	380 kV (UH)		UH-L, 38.7%
	220 kV (H)		H-L, 22.5%
	50 kV (L)		

Impedance diagram

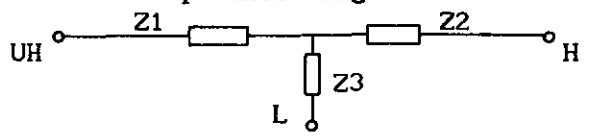

Z1 = 0.21+j44.0 Ω
Z2 = 1.24-j2.74 Ω
Z3 = 1.0 +j67.7 Ω
on 380 kV basis

Short circuit imp. 220 kV network

Z1 = 3.56 + j 35.6 Ω }on 380kV
Z0 = 5.49 + j 54.9 Ω } basis
X0 / X1 = 1.54

Surge Impedance of 220 kV lines

Two double circuit 220 kV lines
Each circuit ; ground mode : 236 Ω
aerial mode : 719 Ω

Resulting feeding network diagram (EMTP-1)

a) positive sequence

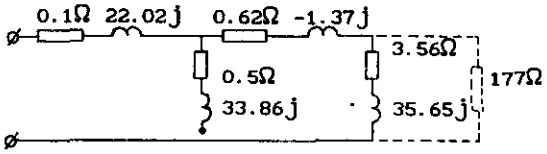

b) zero sequence

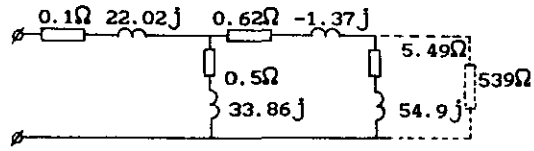

Table of switching moments

The moment t=0 corresponds to the pos.zero-crossing of phase voltage R

field test	phase R [ms]	phase S [ms]	phase T [ms]
K1	18.72	12.06	12.94
K3	2.61	3.28	4.17
K4	15.89	17.56	16.61
K5	15.00	17.33	16.00
K6	6.44	8.39	6.67
K7	1.06	0.67	0.39
K8	12.22	12.72	12.61
K9	12.22	13.11	13.94
K10	2.89	4.11	5.17
K11	2.00	2.94	4.00
K12	4.56	6.89	5.50
K13	14.28	16.83	15.72
K14	7.33	9.00	7.61

Table 2-1

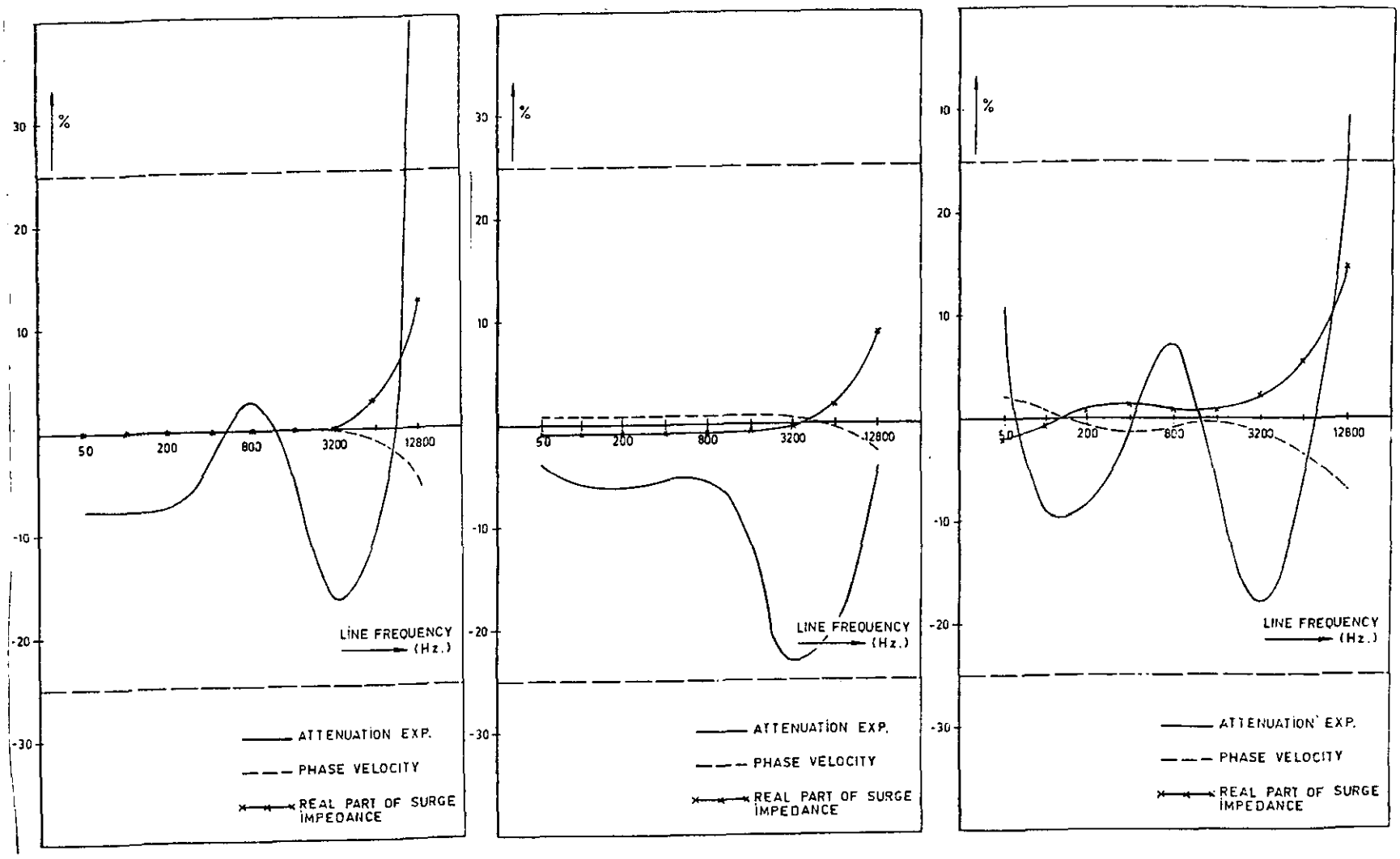

a. Positive-sequence

b. Intercircuit-sequence

c. Zero-sequence

Figure 3-1 . Π -section line model characteristics versus distributed line .

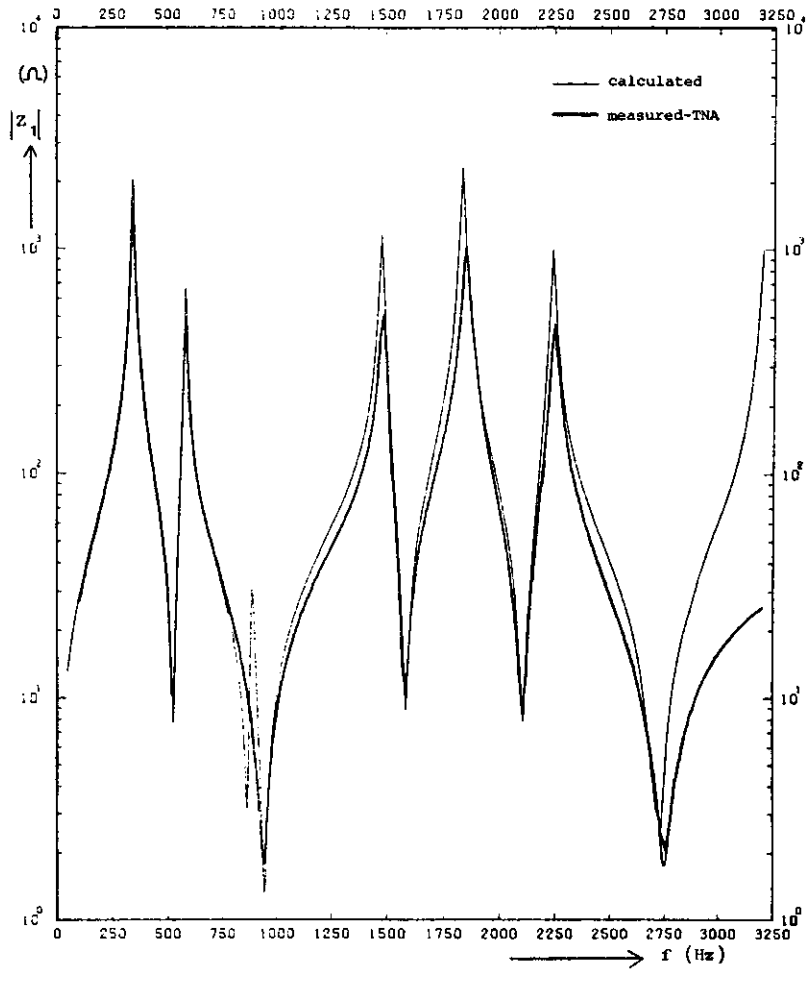

a. Positive-sequence impedance

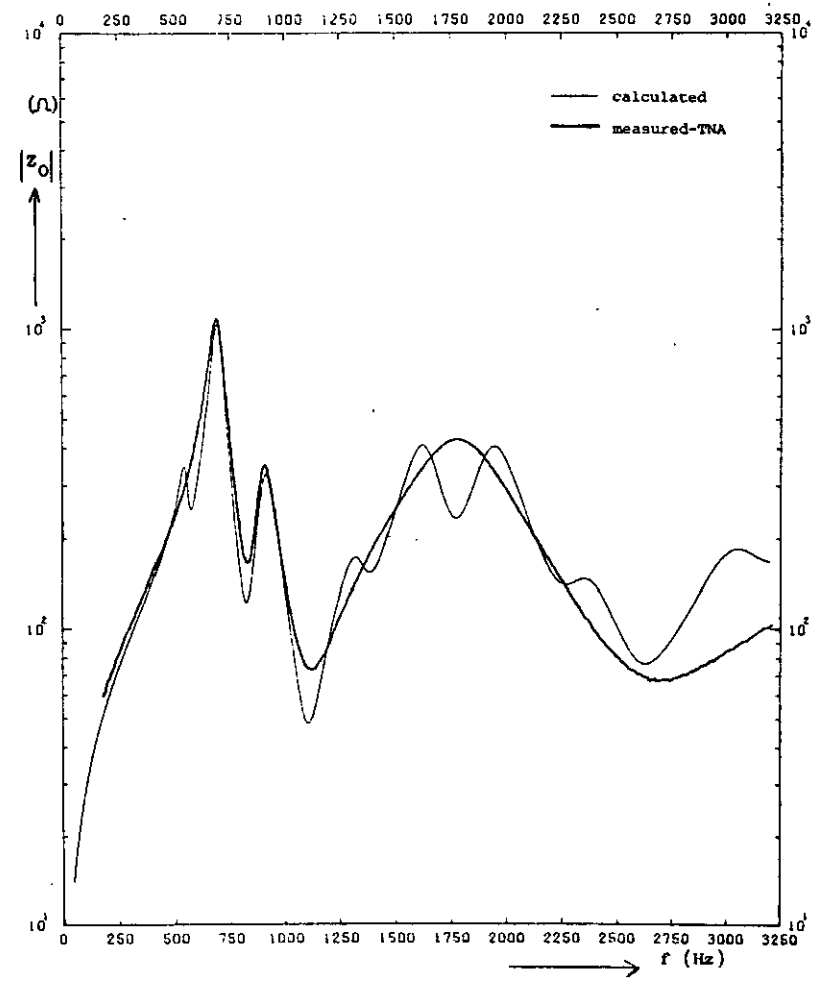

b. Zero-sequence impedance

Figure 3-2 Impedances versus frequency partial network Krimpen

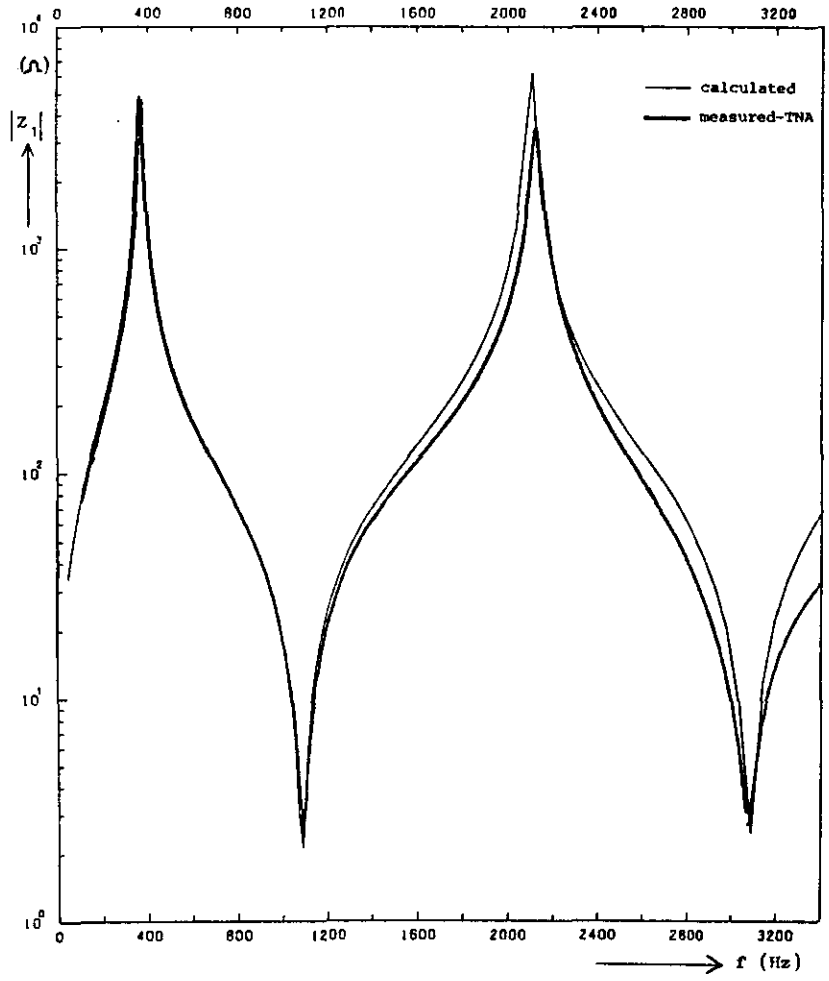

a. Positive-sequence impedance

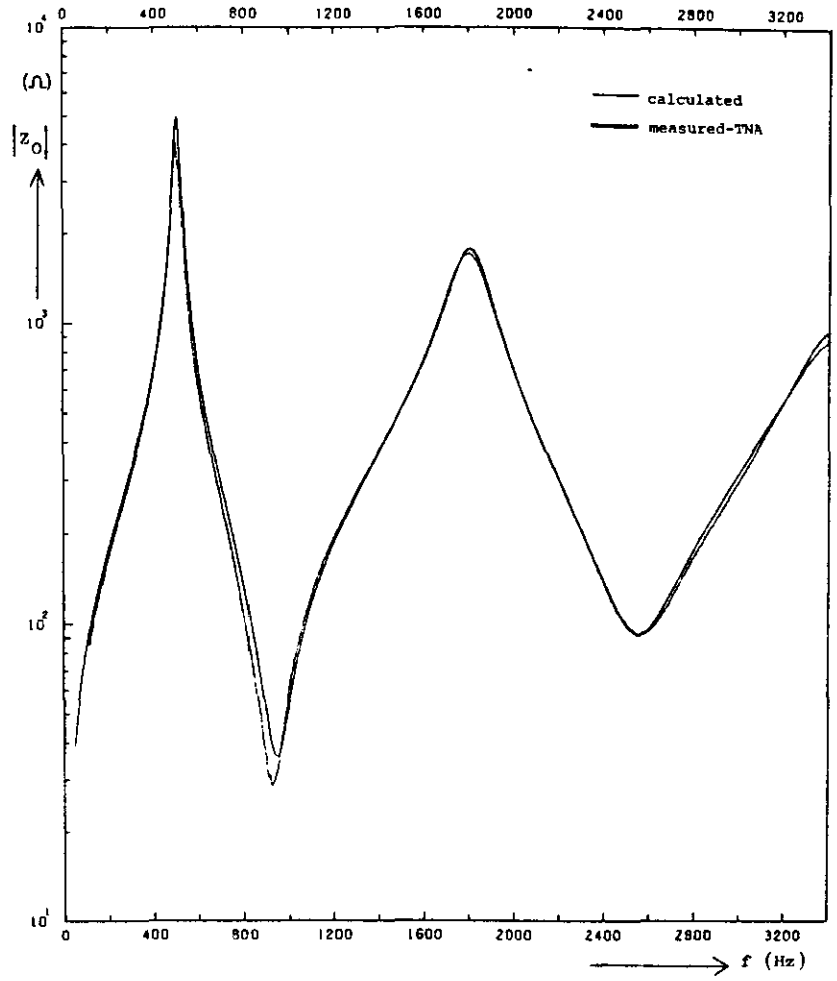

b. Zero-sequence impedance

Figure 3-3 Impedances versus frequency partial network Diemen

Impedance Characteristics

Partial network Krimpen

positive-sequence				zero-sequence			
poles		zeros		poles		zeros	
f(Hz)	|Z| (Ω)	f(Hz)	|Z| (Ω)	f(Hz)	|Z| (Ω)	f(Hz)	|Z| (Ω)
346	2.2 k	530	7.8	696	1.0 k	836	120
586	680	920	1.0	904	330	1106	47
1481	1.2 k	1585	8.8	1750	400	2650	75
1838	2.4 k	2109	7.9				
2238	1.0 k	2725	2.0				

50 Hz : X_1 = 13.2 Ω X_0 = 13.9 Ω

R_1 = 1.18 Ω R_0 = 1.23 Ω

Partial network Diemen

positive-sequence				zero-sequence			
poles		zeros		poles		zeros	
f(Hz)	|Z| (Ω)	f(Hz)	|Z| (Ω)	f(Hz)	|Z| (Ω)	f(Hz)	|Z| (Ω)
364	5.0 k	1085	1.6	507	5.0 k	947	35
2100	6.2 k	3080	2.3	1806	1.75k	2570	90
				3467	900	4300	145

50 Hz : X_1 = 34 Ω X_0 = 39 Ω

R_1 = 3 Ω R_0 = 2 Ω

Data of the equivalent circuits

Partial network Krimpen (f_{tna} = 96 Ω)

pos. sequence ; Foster - II				zero sequence ; Foster -I *)			
branch	L(mH)	C(nF)	R(Ω)	branch	L(mH)	C(nF)	R(Ω)
0	21.5		1.2	0	13.9		
1	62.4	393	7	1	34.7	409	14.1
2	6.0	1336	1	2	6.8	1236	2.8
3	41.2	66	8	3	13.5	166	34.5
4	26.6	57.7	8				
5	3.2	288	2				

Partial network Diemen (f_{tna} = 96 Hz)

pos. sequence ; Foster -II				zero sequence ; Foster -I *)			
branch	L(mH)	C(nF)	R(Ω)	branch	L(mH)	C(nF)	R(Ω)
0	55.1		2.9	0	17.8		
1	8.4	692	1.5	1	145	184	26
2	4.8	150	2.3	2	25	84	28
				3	5.6	102	10

*) Foster -I data equivalent to 3 Z_0

(transformer ratio 1 : 1)

Appendix 4 EMTP input file

```
BEGIN NEW DATA CASE
C EMTP40A INPUT
C
C INSCHAKELEN TWEEDE CIRCUIT KRIMPEN DIEMEN TE DIEMEN
C
C ALLE LIJNEN MET JMARTI PER CIRCUIT GETRANSPONEERD
C SCHAKELMOMENTEN VOLGENS K13-CASE
C 28 OKTOBER 1987
C TWEEDE POGING
C TRANSFORM. IN ENS,VERBETERDE WAARDEN VAN TRAFO EN 220 KV LIJNEN ACHTER ENS
C
C WER FREQUENCY                  STATFR--
POWER FREQUENCY                  .500E+02
C +DELI-IMAX----XOPT----COPT----EPSILN--TOLMAT--TSTART--
   .5E-5    .2E-2 .50E+02 .50E+02
C
+IOUT-IPLOT---IDOUBL--KSSOUT--MAXOUT--IPUN----MEMSAV----ICAT----NENERG--IPRSUP
       1               1               1
C TRANSFORMER AT ENS
C TRANSFORMER BUS3--       IST---PSIST-BUST--RMAG--                          0


  TRANSFORMER                    .1E+01TENS-1
C +CUR----------FLUX-----------
          9999
C BUS1--BUS2--             RK----LK----VOLT--                                0
 1ENS-1                      0.1   22. .1E+01
 2BENS-1                     0.62  -1.4.1E+01
 3DENS-1                     0.5   33.9.1E+01
  TRANSFORMER TENS-1                    TENS-2
 1ENS-2
 2BENS-2
 3DENS-2DENS-1
  TRANSFORMER TENS-1                    TENS-3
 1ENS-3
 2BENS-3
 3      DENS-2
C INFEED AT ENS FROM 150 KV AND 220 KV
C
BUS1--BUS2--BUS3--BUS4--R-----L----------R-----L----------R-----L----------
51BRON-1BENS-1             5.49  54.9
52BRON-2BENS-2             3.56  35.65
53BRON-3BENS-3
C INFEED AT DIEMEN FROM 150 KV
51BRON-1DIM-1R             6.10  61.0
52BRON-2DIM-2R             6.72  67.2
53BRON-3DIM-3R
C INFEED AT KRIMPEN FROM 150 KV
51BRON-1KIJ-1R             6.10  61.0
52BRON-2KIJ-2R             8.34  83.4
53BRON-3KIJ-3R
C INFEED AT CRAYESTEIN FROM 150 KV
51BRON-1CST-1              6.10  61.0
52BRON-2CST-2              121.0 1210.0
53BRON-3CST-3
```

```
C INFEED AT MAASVLAKTE FROM 150 KV AND GENERATOR
51BRON-1MVL-1              2.12  21.2
52BRON-2MVL-2              8.07  80.7
53BRON-3MVL-3
C INFEED AT GEERTRUIDENBERG FROM 150 KV AND GENERATOR
51BRON-1GTB-1              2.54  25.4
52BRON-2GTB-2              5.15  51.5
53BRON-3GTB-3
C INFEED AT EINDHOVEN FROM 150 KV
51BRON-1EHV-1              6.10  61.0
52BRON-2EHV-2              16.13 161.3
53BRON-3EHV-3
C INFEED AT MAASBRACHT FROM 150 KV
51BRON-1MBT-1              1.36  13.64
52BRON-2MBT-2              0.73   7.25
53BRON-3MBT-3
C TRANSMISSIONLINE DIEMEN-ENS USING MARTI-SETUP
-1DIM-1RENS-1                    2.                    -2
      12       .27735291973000000000E+03

      12       .25353064473100000000E-03

-2DIM-2RENS-2                    2.                    -2
      11       .12970094534900000000E+03

      11       .24193117090400000000E-03

-3DIM-3RENS-3                    2.                    -2
      11       .12970094534900000000E+03

      11       .24193117090400000000E-03

C TRANSMISSIONLINE DIEMEN-FAULTPOINT USING MARTI-SETUP
-1DIM-1 FLT-1                    2.                    -2 6
       9       .54196155387000000000E+03

       6       .10458883572500000000E-03

-2DIM-2 FLT-2                    2.                    -2 6
       7       .37854568859400000000E+03

       6       .10044266342700000000E-03

-3DIM-3 FLT-3                    2.                    -2 6
       6       .25923418699600000000E+03

      11       .99550947161600000000E-04

-4DIM-4 FLT-4                    2.                    -2 6
       6       .25923418699600000000E+03

      11       .99550947161600000000E-04

-5DIM-5 FLT-5                    2.                    -2 6
       6       .25923418699600000000E+03

      11       .99550947161600000000E-04

-6DIM-6 FLT-6                    2.                    -2 6
```

```
       6        .259234186996000000000E+03

      11        .995509471616000000000E-04

  0.40824829  0.40824829  0.70710678  0.40824829  0.00000000  0.00000000
  0.00000000  0.00000000  0.00000000  0.00000000  0.00000000  0.00000000
  0.40824829  0.40824829 -0.70710678  0.40824829  0.00000000  0.00000000
  0.00000000  0.00000000  0.00000000  0.00000000  0.00000000  0.00000000
  0.40824829  0.40824829  0.00000000 -0.81649658  0.00000000  0.00000000
  0.00000000  0.00000000  0.00000000  0.00000000  0.00000000  0.00000000
  0.40824829 -0.40824829  0.00000000  0.00000000  0.70710678  0.40824829
  0.00000000  0.00000000  0.00000000  0.00000000  0.00000000  0.00000000
  0.40824829 -0.40824829  0.00000000  0.00000000 -0.70710678  0.40824829
  0.00000000  0.00000000  0.00000000  0.00000000  0.00000000  0.00000000
  0.40824829 -0.40824829  0.00000000  0.00000000  0.00000000 -0.81649658
  0.00000000  0.00000000  0.00000000  0.00000000  0.00000000  0.00000000
C TRANSMISSIONLINE FAULTPOINT-KRIMPEN USING JMARTI-SETUP
-1FLT-1 KIJ-1 DIM-1 FLT-1      2.                        -2 6
-2FLT-2 KIJ-2 DIM-2 FLT-2      2.                        -2 6
-3FLT-3 KIJ-3 DIM-3 FLT-3      2.                        -2 6
-4FLT-4 KIJ-4 DIM-4 FLT-4      2.                        -2 6
-5FLT-5 KIJ-5 DIM-5 FLT-5      2.                        -2 6
-6FLT-6 KIJ-6 DIM-6 FLT-6      2.                        -2 6
C TRANSMISSIONLINE KRIMPEN-CRAYESTEIN USING JMARTI
-1KIJ-1RCST-1                  2.                        -2
      12        .273890590134000000000E+03

      11        .508439638485000000000E-04

-2KIJ-2RCST-2                  2.                        -2
      10        .116278796129000000000E+03

      10        .504368921206000000000E-04

-3KIJ-3RCST-3                  2.                        -2
      10        .116278796129000000000E+03

      10        .504368921206000000000E-04

C TRANSMISSIONLINE CRAYESTEIN-MAASVLAKTE USING JMARTI
-1MVL-1 CST-1                  2.                        -2
      12        .273890590134000000000E+03

      12        .234913021531000000000E-03

-2MVL-2 CST-2                  2.                        -2
      10        .116278796129000000000E+03

      12        .225612999781000000000E-03

-3MVL-3 CST-3                  2.                        -2
      10        .116278796129000000000E+03

      12        .225612999781000000000E-03

C TRANSMISSIONLINE KRIMPEN-GEERTRUIDENBERG USING JMARTI-SETUP
-1KIJ-1RGTB-1                  2.                        -2
      12        .277352919730000000000E+03
```

```
      11        .1138069400900000000E-03

-2KIJ-2RGTB-2                    2.                        -2
      11        .1297009453490000000E+03

      11        .1108870563090000000E-03

-3KIJ-3RGTB-3                    2.                        -2
      11        .1297009453490000000E+03

      11        .1108870563090000000E-03

C TRANSMISSIONLINE GEERTRUIDENBERG-EINDHOVEN USING JMARTI-SETUP
-1GTB-1 EHV-1                    2.                        -2
      12        .2434660496240000000E+03

      12        .2271439815710000000E-03

-2GTB-2 EHV-2                    2.                        -2
      13        .9846004601200000000E+02

      11        .2193707521760000000E-03

-3GTB-3 EHV-3                    2.                        -2
      13        .9846004601200000000E+02

      11        .2193707521760000000E-03

C TRANSMISSIONLINE EINDHOVEN-MAASBRACHT USING JMARTI-SETUP
-1EHV-1 MBT-1                    2.                        -2
      12        .2773529197300000000E+03

      12        .1692148040560000000E-03

-2EHV-2 MBT-2                    2.                        -2
      11        .1297009453490000000E+03

      12        .1633672364330000000E-03

-3EHV-3 MBT-3                    2.                        -2
      11        .1297009453490000000E+03

      12        .1633672364330000000E-03

C TRANSMISSIONLINES (5) MAASBRACHT -DODEWAARD,-BELGIUM,AND GERMANY USING
WAVE-IMPEDANCE
51BRON-1MBT-1              153.3
52BRON-2MBT-2               52.5
53BRON-3MBT-3
C TRANSMISSIONLINES 220 KV BEHIND ENS (4)
51BRON-1BENS-1             539.
52BRON-2BENS-2             177.
53BRON-3BENS-3
BLANK CARD TERMINATING BRANCHES
C SWITCHES AT DIEMEN
C BUS1--BUS2--TCLOSE----TOPEN-----IEPS------                                  0


  DIM-1RDIM-1 -.2000E-01 .2000E-01
```

```
  DIM-2RDIM-2 -.2000E-01 .2000E-01
  DIM-3RDIM-3 -.2000E-01 .2000E-01
  DIM-1RDIM-4 -.0000E-03 .2000E-01
  DIM-2RDIM-5 -.2556E-02 .2000E-01
  DIM-3RDIM-6 -.1444E-02 .2000E-01
C SWITCHES AT KRIMPEN
  KIJ-1RKIJ-1 -.2000E-01 .2000E-01
  KIJ-2RKIJ-2 -.2000E-01 .2000E-01
  KIJ-3RKIJ-3 -.2000E-01 .2000E-01
C KIJ-1RKIJ-4 -.2000E-01 .2000E-01                                          1


C KIJ-2RKIJ-5 -.2000E-01 .2000E-01                                          1


C KIJ-3RKIJ-6 -.2000E-01 .2000E-01                                          1


BLANK CARD TERMINATING SWITCHES
C SOURCE
C BUS1--I-AMPL------FREQ------PHI-------                    TSTART----TSTOP---
14BRON-1 0 .3190E+06 .5000E+02       167         0                  -1
14BRON-2 0 .3190E+06 .5000E+02        47         0                  -1
14BRON-3 0 .3190E+06 .5000E+02       -73         0                  -1
BLANK CARD TERMINATING SOURCES
NAM1--NAM2--NAM3--NAM4--NAM5--NAM6--NAM7--NAM8--NAM9--NAM10-NAM11-NAM12-NAM13-
C  DIM-1 DIM-2 DIM-3 DIM-4 DIM-5 DIM-6
C  FLT-1 FLT-2 FLT-3 FLT-4 FLT-5 FLT-6
  KIJ-4 KIJ-5 KIJ-6
  ENS-1 ENS-2 ENS-3
  GTB-1 GTB-2 GTB-3
  CST-1 CST-2 CST-3
BLANK CARD TERMINATING OUTPUT
BLANK CARD TERMINATING PLOT-REQUESTS
BEGIN NEW DATA CASE
BLANK CARD TERMINATING EMTP RUN
```

Eindhoven University of Technology Research Reports
Faculty of Electrical Engineering

ISSN 0167-9708
Coden: TEUEDE

(171) Monnee, P. and M.H.A.J. Herben
MULTIPLE-BEAM GROUNDSTATION REFLECTOR ANTENNA SYSTEM: A preliminary study.
EUT Report 87-E-171. 1987. ISBN 90-6144-171-4

(172) Bastiaans, M.J. and A.H.M. Akkermans
ERROR REDUCTION IN TWO-DIMENSIONAL PULSE-AREA MODULATION, WITH APPLICATION TO COMPUTER-GENERATED TRANSPARENCIES.
EUT Report 87-E-172. 1987. ISBN 90-6144-172-2

(173) Zhu Yu-Cai
ON A BOUND OF THE MODELLING ERRORS OF BLACK-BOX TRANSFER FUNCTION ESTIMATES.
EUT Report 87-E-173. 1987. ISBN 90-6144-173-0

(174) Berkelaar, M.R.C.M. and J.F.M. Theeuwen
TECHNOLOGY MAPPING FROM BOOLEAN EXPRESSIONS TO STANDARD CELLS.
EUT Report 87-E-174. 1987. ISBN 90-6144-174-9

(175) Janssen, P.H.M.
FURTHER RESULTS ON THE McMILLAN DEGREE AND THE KRONECKER INDICES OF ARMA MODELS.
EUT Report 87-E-175. 1987. ISBN 90-6144-175-7

(176) Janssen, P.H.M. and P. Stoica, T. Söderström, P. Eykhoff
MODEL STRUCTURE SELECTION FOR MULTIVARIABLE SYSTEMS BY CROSS-VALIDATION METHODS.
EUT Report 87-E-176. 1987. ISBN 90-6144-176-5

(177) Stefanov, B. and A. Veefkind, L. Zarkova
ARCS IN CESIUM SEEDED NOBLE GASES RESULTING FROM A MAGNETICALLY INDUCED ELECTRIC FIELD.
EUT Report 87-E-177. 1987. ISBN 90-6144-177-3

(178) Janssen, P.H.M. and P. Stoica
ON THE EXPECTATION OF THE PRODUCT OF FOUR MATRIX-VALUED GAUSSIAN RANDOM VARIABLES.
EUT Report 87-E-178. 1987. ISBN 90-6144-178-1

(179) Lieshout, G.J.P. van and L.P.P.P. van Ginneken
GM: A gate matrix layout generator.
EUT Report 87-E-179. 1987. ISBN 90-6144-179-X

(180) Ginneken, L.P.P.P. van
GRIDLESS ROUTING FOR GENERALIZED CELL ASSEMBLIES: Report and user manual.
EUT Report 87-E-180. 1987. ISBN 90-6144-180-3

(181) Bollen, M.H.J. and P.T.M. Vaessen
FREQUENCY SPECTRA FOR ADMITTANCE AND VOLTAGE TRANSFERS MEASURED ON A THREE-PHASE POWER TRANSFORMER.
EUT Report 87-E-181. 1987. ISBN 90-6144-181-1

(182) Zhu Yu-Cai
BLACK-BOX IDENTIFICATION OF MIMO TRANSFER FUNCTIONS: Asymptotic properties of prediction error models.
EUT Report 87-E-182. 1987. ISBN 90-6144-182-X

(183) Zhu Yu-Cai
ON THE BOUNDS OF THE MODELLING ERRORS OF BLACK-BOX MIMO TRANSFER FUNCTION ESTIMATES.
EUT Report 87-E-183. 1987. ISBN 90-6144-183-8

(184) Kadete, H.
ENHANCEMENT OF HEAT TRANSFER BY CORONA WIND.
EUT Report 87-E-184. 1987. ISBN 90-6144-6

(185) Hermans, P.A.M. and A.M.J. Kwaks, I.V. Bruza, J. Dijk
THE IMPACT OF TELECOMMUNICATION ON RURAL AREAS IN DEVELOPING COUNTRIES.
EUT Report 87-E-185. 1987. ISBN 90-6144-185-4

(186) Fu Yanhong
THE INFLUENECE OF CONTACT SURFACE MICROSTRUCTURE ON VACUUM ARC STABILITY AND ARC VOLTAGE.
EUT Report 87-E-186. 1987. ISBN 90-6144-186-2

(187) Kaiser, F. and L. Stok, R. van den Born
DESIGN AND IMPLEMENTATION OF A MODULE LIBRARY TO SUPPORT THE STRUCTURAL SYNTHESIS.
EUT Report 87-E-187. 1987. ISBN 90-6144-187-0

Eindhoven University of Technology Research Reports
Faculty of Electrical Engineering

ISSN 0167-9708
Coden: TEUEDE

(188) Jóźwiak, J.
THE FULL DECOMPOSITION OF SEQUENTIAL MACHINES WITH THE STATE AND OUTPUT BEHAVIOUR REALIZATION.
EUT Report 88-E-188. 1988. ISBN 90-6144-188-9

(189) Pineda de Gyvez, J.
ALWAYS: A system for wafer yield analysis.
EUT Report 88-E-189. 1988. ISBN 90-6144-189-7

(190) Siuzdak, J.
OPTICAL COUPLERS FOR COHERENT OPTICAL PHASE DIVERSITY SYSTEMS.
EUT Report 88-E-190. 1988. ISBN 90-6144-190-0

(191) Bastiaans, M.J.
LOCAL-FREQUENCY DESCRIPTION OF OPTICAL SIGNALS AND SYSTEMS.
EUT Report 88-E-191. 1988. ISBN 90-6144-191-9

(192) Worm, S.C.J.
A MULTI-FREQUENCY ANTENNA SYSTEM FOR PROPAGATION EXPERIMENTS WITH THE OLYMPUS SATELLITE.
EUT Report 88-E-192. 1988. ISBN 90-6144-192-7

(193) Kersten, W.F.J. and G.A.P. Jacobs
ANALOG AND DIGITAL SIMULATION OF LINE-ENERGIZING OVERVOLTAGES AND COMPARISON WITH MEASUREMENTS IN A 400 kV NETWORK.
EUT Report 88-E-193. 1988. ISBN 90-6144-193-5

(194) Hosselet, L.M.L.F.
MARTINUS VAN MARUM: A Dutch scientist in a revolutionary time.
EUT Report 88-E-194. 1988. ISBN 90-6144-194-3

(195) Bondarev, V.N.
ON SYSTEM IDENTIFICATION USING PULSE-FREQUENCY MODULATED SIGNALS.
EUT Report 88-E-195. 1988. ISBN 90-6144-195-1

(196) Liu Wen-Jiang, Zhu Yu-Cai and Cai Da-Wei
MODEL BUILDING FOR AN INGOT HEATING PROCESS: Physical modelling approach and identification approach.
EUT Report 88-E-196. 1988. ISBN 90-6144-196-X